Control Engineering Practice 90 (2019) 50–62

Contents lists available at ScienceDirect

Control Engineering Practice

journal homepage: www.elsevier.com/locate/conengprac

Permanent magnet DC motor parameters estimation via universal adaptive stabilization

Hafiz M. Usman, Shayok Mukhopadhyay *, Habibur Rehman

American University of Sharjah, Department of Electrical Engineering, P.O. Box 26666, Sharjah, United Arab Emirates

ARTICLE INFO

Keywords:
Universal adaptive stabilizer
Adaptive parameters estimation
Permanent magnet DC motor

ABSTRACT

This paper presents a quick and effective adaptive estimation methodology for parameters estimation of a permanent magnet (PM) DC motor. The proposed technique uses a universal adaptive stabilizer (UAS). This technique estimates PMDC motor parameters in a single experimental run using input voltage, current and speed. Over time, due to aging and wear, a motor's parameters values do not match those in the datasheet. Mathematical proofs, experimental results supporting the proposed approach are presented. Despite the persistence of excitation condition not being imposed, the proposed technique produces good results, and is verified in earlier work on Li-ion battery parameters estimation.

1. Introduction

DC motors are used in several fields e.g. robotics, consumer electronics, and industrial control. Parameters of a DC motor, provided by a manufacturer, can work very well for a new motor. However, DC motor parameters vary due to aging and related wear and tear. Thus accuracy of a DC motor model can be improved by updating motor parameters as a motor ages. This motivated the authors to design an adaptive parameter estimator for a PMDC motor.

Different DC motor parameters estimation strategies are available in the literature (Sendrescu, 2012)-(Wu, 2010). The method in Wu (2010) presents a power series expansion approach to estimate the electrical and mechanical time constants, and torques due to friction for a DC motor. The speed response with a step voltage excitation, followed by curve fitting, is used to compute the power series coefficients related to DC motor parameters (Wu, 2010). A flower pollination based meta-heuristic optimization routine with step input excitation is used in Puangdownreong, Hlungnamtip, Thammarat, and Nawikavatan (2017), for DC motor parameters identification. Accuracy assessment of PMDC motor parameters, estimated by using different bio-inspired optimization algorithms such as particle swarm, ant colony, and artificial bee colony optimization methods, is presented in Sankardoss and Geethanjali (2017). Convergence analysis and number of iterations required for the aforementioned bio-inspired optimization algorithms are also detailed in Sankardoss and Geethanjali (2017). A hybrid sliding mode observer is analyzed for simultaneous estimation of speed, and the time varying DC series motor torque parameter (K_t), under external disturbance. A recursive least squares based approach is used in Sun, Li, Li, Shi, and Hu (2015) for real-time parameters identification of a brushless DC motor. An adaptive learning method which accelerates the online training of a neural network is outlined in Rubaai and Kotaru (2000). The method in Rubaai and Kotaru (2000) absorbs system uncertainties, and estimates DC motor parameters. The motor transfer function technique (Da Silva, Bastos, Da Silva Casillo, & Casillo, 2016), and moment method (Hadef, Bourouina, & Mekideche, 2008), require several experimentations to effectively identify DC motor parameters. The online identification of viscous friction, and motor inertia for a servo motor using an open-loop algebraic method, is presented in Mamani, Becedas, Feliu-Batlle, and Sira-Ramirez (2007). The method in Mamani et al. (2007) requires input voltage and angular position measurements of a DC servo motor for simultaneous determination of viscous friction and motor inertia. The optimization of a PI controller is utilized in Galijašević, Mašić, Smaka, Akšamović, and Balić (2011) for DC motor digital control and parameters estimation. A distribution based offline parameters identification approach, outlined in Sendrescu (2012), transforms a system of linear differential equations into linear algebraic equations. This method utilizes discrete-time data and identifies parameters of a continuous-time model. But the method in Sendrescu (2012) may be sensitive to the sampling rate of the motor speed and current. Unlike (Da Silva et al., 2016; Galijašević et al., 2011; Hadef et al., 2008; Puangdownreong et al., 2017; Sankardoss & Geethanjali, 2017), the UAS based adaptive estimation strategy, proposed in this paper, minimizes the required experimental effort, as a result the estimated parameters converge to near accurate values within a single experimental run.

Extensive research work exists on parameters estimation strategies in general. The authors in Ortega, Praly, Aranovskiy, Yi, and Zhang (2018) develop a novel parameters estimation technique based on a dynamic regressor extension and mixing (DREM) method. This technique

* Corresponding author.
E-mail addresses: b00071330@aus.edu (H.M. Usman), smukhopadhyay@aus.edu (S. Mukhopadhyay), rhabib@aus.edu (H. Rehman).

https://doi.org/10.1016/j.conengprac.2019.06.006
Received 4 November 2018; Received in revised form 12 June 2019; Accepted 13 June 2019
Available online xxxx
0967-0661/

is proven to perform better compared to gradient-based and least-squares estimators. Further performance enhancement of the DREM strategy is reported in Aranovskiy, Bobtsov, Ortega, and Pyrkin (2017) and Belov, Aranovskiy, Ortega, Barabanov, and Bobtsov (2018). The use of signal injection techniques to simplify the complexity of parameter estimation-based observers (PEBO) is presented in Yi, Ortega, and Zhang (2018). A sensorless controller is formulated using this method for magnetic levitation systems and the results are verified through numerical simulations (Yi et al., 2018). A new approach for partial state identification of nonlinear systems, based on parameter identification, is reported in Ortega, Bobtsov, Pyrkin, and Aranovskiy (2015). Recently, an adaptive parameter estimation strategy is introduced in Na, Xing, and Costa-Castelló (2018) for nonlinear systems with unknown time-varying parameters. The adaptive scheme in Na et al. (2018) utilizes input and output measurements for parameters estimation, and is verified against gradient-based and least-squares algorithms. Further, the robustness of this method is experimentally validated on a roto-magnet plant under bounded disturbance.

In this work, a novel UAS based adaptive parameters estimation method is proposed for PMDC motors. This UAS based adaptive estimation strategy (Ali, Mukhopadhyay, Rehman, & Khurram, 2017), is known to converge quickly, requires less experimental effort, and estimates Lithium-ion battery model parameters with good accuracy. Thus motivated, the adaptive parameters estimation method from Ali et al. (2017) is chosen for the work in this paper. Another motivation for this work is an observation that DC motor parameters change over the operational life of a motor, and so a strategy that can run quickly in a small period of routine operational downtime that a motor may have, is attractive. The adaptive parameters estimation technique from Ali et al. (2017) used in this work requires the input voltage, current and speed measured at no-load condition. This work is the first attempt, to the best of the authors' knowledge, to employ a UAS based high-gain adaptive observer for parameters estimation of a PMDC motor. The work in Ali et al. (2017) requires prior offline experimentation for determining certain parameters, namely the open circuit voltage parameters, and also requires some post-processing to estimate the battery series resistance. This is due to the complex structure of a detailed battery model, and also due to the corresponding structure of the UAS based observer proposed for the above task. Unlike (Ali et al., 2017), this work, however, does not require any prior offline experimentation or any post-processing. Thus, estimates of all the DC motor parameters are obtained in a single experimental run. Further, the observer in Ali et al. (2017) does not use the input i.e. the battery discharge current in the key state equations, but only uses an adaptively computed signal as input to these key state equations of an adaptive observer. In this work, the structure of the observer is significantly different compared to Ali et al. (2017) because the nature of the parameters, and the manner in which these parameters enter the model equations, are vastly different compared to Ali et al. (2017). Further, this work also utilizes the actual motor current, and speed, along with an adaptively computed signal, as inputs to the proposed observer. Thus, the details concerning the results in this manuscript are different from Ali et al. (2017), even if the overall structure of the results may appear similar.

Also, the formulation of the observer used for parameter estimation is very different from the standard gradient based, or least squares based parameter identification techniques as in Sastry (1999). To emphasize the difference, it is worth considering the fact that the input to the observer, proposed in this paper, is a Nussbaum type switching function, of Mittag-Leffler form. By the definition of a Nussbaum function from Ilchmann (1993), it can be readily seen that such an input to the observer must oscillate rapidly, and the frequency of such oscillations must change. Further an alternative but equivalent statement of the persistence of excitation (PE) condition from Sastry (1999) is that the "input signal has as many sinusoids as there are unknown parameters", and by the definition of a Nussbaum function, and given its varying frequency, the above condition is readily achieved. Theoretically considering the details related to the requirement of imposition of the PE condition, are very far beyond the scope of the current manuscript, and are left for future investigation. It is however interesting to note that some work involving other techniques which do not impose PE, already exists (Aranovskiy et al., 2017). Thus it is possible, as in Aranovskiy et al. (2017) to not impose PE and achieve reliable parameter estimates. And the UAS based approach proposed in this paper has been verified through extensive experimentation in Ali et al. (2017), and results show satisfactory parameter estimation, without explicitly requiring PE to hold. Further the UAS based technique has been observed to operate well even in the presence of noise in Ali et al. (2017), Al Khatib, Al-Masri, Mukhopadhyay, Jaradat, and Abdel-Hafez (2015), Alkhawaja et al. (2018), Mukhopadhyay and Zhang (2014) and Mukhopadhyay, Li, and Chen (2008). And similar to Ali et al. (2017) and Mukhopadhyay and Zhang (2014), this work uses UAS for estimation purposes, so any noise or disturbances can be simply eliminated by using appropriate pre-filtering before the proposed technique is used. The choice of using a Nussbaum function of Mittag-Leffler type is also a deliberate one, because as seen in Mukhopadhyay et al. (2008), such a Nussbaum function outperforms other known variants in terms of speed of convergence of the error to zero. This is also observed for the current work, and is also shown by appropriate results presented later in the paper. The results in this paper are derived for motor operation on no load, and while investigation of motor loading on parameters estimation by the approach proposed in this work is left for future efforts, the following is worth consideration. As noted by the results presented in Sankardoss and Geethanjali (2017), PMDC motor parameters are invariant to loading.

This paper is organized as follows. Background information is discussed in Section 2. The proposed UAS based high gain adaptive observer for PMDC motor parameters estimation, is formulated in Section 3. Section 4 provides the mathematical justification of the proposed method. Experimental results for DC motor parameters estimation are detailed in Section 5. Concluding remarks are presented in Section 6 of this paper.

2. Background

This section gives a brief review of PMDC motor modeling, and basics related to the Universal Adaptive Stabilizer (UAS).

2.1. Permanent magnet DC motor modeling

The equivalent circuit of a PMDC motor is illustrated in Fig. 1. The magnitude and polarity of the supply voltage $E(t)$ determine the motor speed and direction of rotation. The motor electrical components, as shown in Fig. 1, are armature resistance, armature inductance and fixed magnetic field winding. In a PMDC motor, the field winding consists of permanent magnets on the stator. The rotor moment of inertia and viscous friction form the mechanical components of Fig. 1. The current and speed dynamics of a PMDC motor at no-load are expressed by (1) and (2).

Eqs. (1) and (2) are derived from Hernández-Márquez, Silva-Ortigoza, García-Sánchez, Marcelino-Aranda, and Saldaña-González (2018), Rodríguez-Molina, Villarreal-Cervantes, Álvarez-Gallegos, and Aldape-Pérez (2019), Sankardoss and Geethanjali (2017) and Silva-Ortigoza, Hernández-Guzmán, Antonio-Cruz, and Munoz-Carrillo (2015) at no load condition, i.e. $\tau = 0$. Where τ represents the load torque. Note that the back electromotive force factor is represented by $K_b\omega(t)$ in (1).

$$L_a \frac{di_a(t)}{dt} = E(t) - R_a i_a(t) - K_b\omega(t) \tag{1}$$

$$J \frac{d\omega(t)}{dt} = K_t i_a(t) - b\omega(t) \tag{2}$$

Here $E(t)$ is the input voltage (V), i_a is the armature circuit current (A), R_a represents equivalent armature circuit resistance (Ohm), L_a

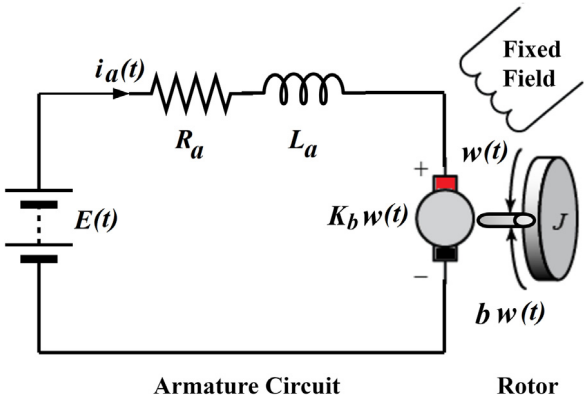

Fig. 1. Electromechanical representation of a PMDC motor system.

represents armature inductance (H), K_b is the back EMF constant (V s/rad), $\omega(t)$ is the speed (rad/s), J is the rotor moment of inertia (kg m^2), K_t is the torque constant (N m/A) and b is the coefficient of viscous friction (N m s/rad).

2.2. Universal Adaptive Stabilizer (UAS)

Nussbaum functions are a class of switching functions, which are commonly used in high-gain adaptive control, namely Universal Adaptive Stabilization (UAS) (Ilchmann, 1993). UAS strategies are commonly used if, not-only are the parameters of a system unknown, but the correct sign of the control input is also unknown (Ilchmann, 1993). A UAS based strategy therefore quickly searches for, and establishes the right magnitude and sign of the 'control' signal required. A Mittag-Leffler (ML) type of Nussbaum function, when used within a UAS scheme, is known to do so quicker compared to other available Nussbaum functions (Li & Chen, 2009; Mukhopadhyay et al., 2008). Some of the advantages of using Nussbaum type switching functions with UAS include the ability to control systems having complex and uncertain, or even unstable dynamics, i.e. the asymptotic stability of a system can be guaranteed even without having any knowledge of the system parameters magnitude or sign (Ilchmann, 1993; Li & Chen, 2009). When used with parameter estimation schemes, UAS is useful, because incorrect choices of parameters (chosen by the estimation process) can lead to an unstable observer, which UAS helps recover from. This concept has been successfully utilized in Ali et al. (2017), Mukhopadhyay and Zhang (2014) and Usman, Mukhopadhyay, and Rehman (2018). The ML function shown in (3) is mostly used in the solution of fractional order equations (Mathai & Haubold, 2008). In this paper, the ML function in (3) is used as a Nussbaum type switching function (Ali et al., 2017; Mukhopadhyay & Zhang, 2014).

$$E_\alpha(z) = \sum_{k=0}^{\infty} \frac{z^k}{\Gamma(k\alpha+1)} \tag{3}$$

In Eq. (3), $\Gamma(z+1) = z\Gamma(z), z > 0$ describes the standard Gamma function. A Nussbaum function is a piecewise right continuous function $N(\cdot) : [k', \infty) \to \mathbb{R}$ satisfying (4) and (5) (Ilchmann, 1993).

$$\sup_{k>k_0} \frac{1}{k-k_0} \int_{k_0}^{k} N(\tau)d\tau = +\infty \tag{4}$$

$$\inf_{k>k_0} \frac{1}{k-k_0} \int_{k_0}^{k} N(\tau)d\tau = -\infty \tag{5}$$

For some $k_0 \in [k', \infty)$, if $\alpha \in (2, 3]$ and $\lambda > 0$, then the ML function $E_\alpha(-\lambda t^\alpha)$ is Nussbaum function (Li & Chen, 2009). In (3)–(5), k, k_0, and $k' \in \mathbb{R}$. The MATLAB implementation of the ML function as a Nussbaum type switching function (Mukhopadhyay, 2008), is shown in Fig. 2.

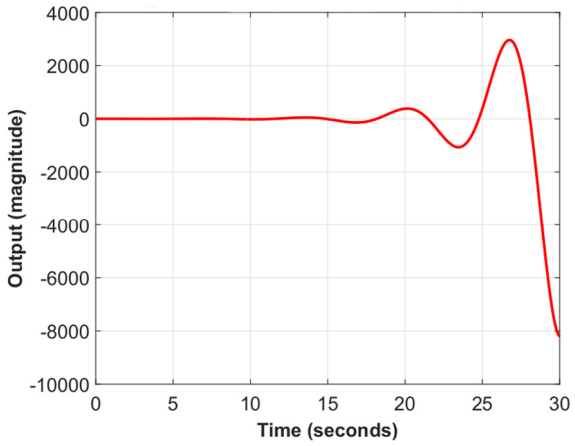

Fig. 2. Mittag Leffler function $E_\alpha(-\lambda t^\alpha)$ as a Nussbaum type switching function for $\lambda = 1$ and $\alpha = 2.5$.

3. UAS based high gain adaptive observer for PMDC motor parameters estimation

The PMDC motor equations (1) and (2) are used to form a novel UAS based high-gain adaptive estimator, as shown by (6)–(7). These are used for DC motor parameters estimation. The actual source voltage $E(t)$ and speed $\omega(t)$ are used in (6), whereas the actual input current $i_a(t)$ is used in (7) for adaptive parameters estimation.

$$\hat{L}_a(t)\frac{d\hat{i}_a(t)}{dt} = E(t) - \hat{R}_a(t)\hat{i}_a(t) - \hat{K}_b(t)\omega(t) + \hat{L}_a(t)u_1(t),\ \hat{i}_a(t) \geq 0 \text{ for } t \geq t_0, \tag{6}$$

$$\hat{J}(t)\frac{d\hat{\omega}(t)}{dt} = \hat{K}_t(t)i_a(t) - \hat{b}(t)\hat{\omega}(t) + \hat{J}(t)u_2(t),\ \hat{\omega}(t) \geq 0 \text{ for } t \geq t_0. \tag{7}$$

Here $\hat{i}_a(t)$, $\hat{\omega}(t) \in \mathbb{R}$ are the estimated armature circuit current and motor speed respectively. Also, $\hat{L}_a(t)$, $\hat{R}_a(t)$, $\hat{K}_b(t)$, $\hat{K}_t(t)$, $\hat{J}(t)$, $\hat{b}(t) \in \mathbb{R}$, represent the estimated equivalent armature circuit inductance, resistance, back EMF constant, torque constant, rotor moment of inertia, and viscous friction coefficient of a PMDC motor respectively. Compared to (1)–(2), the observer equations (6)–(7) have some extra terms. These terms are required to make the motor current and speed estimation errors approach zero overtime. The input $u_1(t)$ for (6) is given by (11).

$$e_1(t) = i_a(t) - \hat{i}_a(t) \tag{8}$$

$$\dot{k}_1(t) = e_1^2(t),\ k_1(t_0) = k_{10} > 0 \tag{9}$$

$$N(k_1(t)) = E_\alpha(-\lambda k_1(t)^\alpha) \tag{10}$$

$$u_1(t) = N(k_1(t))e_1(t) \tag{11}$$

The input $u_2(t)$ for (7) is given in (15).

$$e_2(t) = \omega(t) - \hat{\omega}(t) \tag{12}$$

$$\dot{k}_2(t) = e_2^2(t),\ k_2(t_0) = k_{20} > 0 \tag{13}$$

$$N(k_2(t)) = E_\alpha(-\lambda k_2(t)^\alpha) \tag{14}$$

$$u_2(t) = N(k_2(t))e_2(t) \tag{15}$$

In (10), and (14) $\lambda = 1$, and $\alpha = 2.5$, thus resulting in a Nussbaum type switching function of ML form to be used in producing the signals $u_1(t)$ and $u_2(t)$. Furthermore, Eq. (16) is used to estimate the parameters of the PMDC motor described in (6)–(7), where $\hat{z}_n(t) \in \mathbb{R}, \hat{z}_n(t) > 0$, $n \in \{1, 2, \ldots, 6\}$.

$$\dot{\hat{z}}_n(t) = e^2(t) + \lambda_{xn}(z_{nu} - \hat{z}_n(t)) + \lambda_{yn}(z_{nl} - \hat{z}_n(t)), \tag{16}$$

where

$$e(t) = e_1(t),\ \text{if } n \in \{1, 2, 3\}, \tag{17}$$

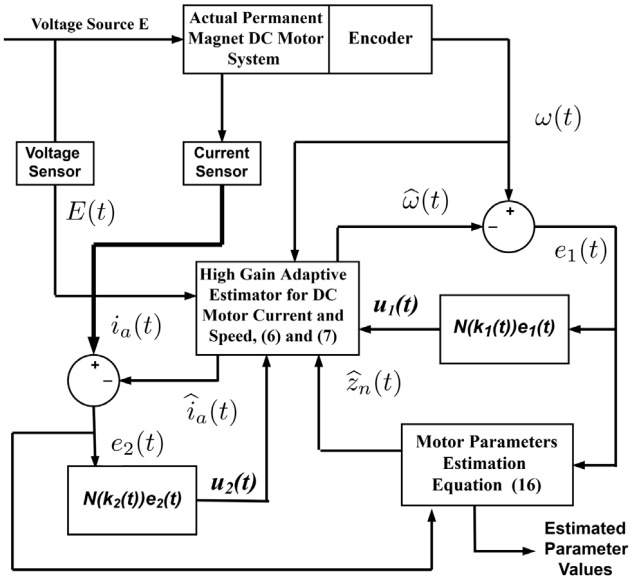

Fig. 3. Flowchart of UAS based adaptive parameters estimation of PMDC motor system.

$$e(t) = e_2(t), \text{ if } n \in \{4,5,6\}. \tag{18}$$

The PMDC motor parameters $\hat{L}_a(t)$, $\hat{R}_a(t)$, $\hat{K}_b(t)$, $\hat{J}(t)$, $\hat{b}(t)$, $\hat{K}_t(t)$ are represented by $\hat{z}_1(t)$, $\hat{z}_2(t)$, $\hat{z}_3(t)$, $\hat{z}_4(t)$, $\hat{z}_5(t)$, $\hat{z}_6(t)$ respectively. For $n \in \{1,2,3\}$, $e(t) = e_1(t)$ in (16), and for $n \in \{4,5,6\}$, $e(t) = e_2(t)$ in (16). That is $e_1(t)$ is used to estimate $\hat{L}_a(t)$, $\hat{R}_a(t)$, $\hat{K}_b(t)$, and $e_2(t)$ is used to estimate $\hat{J}(t)$, $\hat{b}(t)$, $\hat{K}_t(t)$ in (16) respectively. The adaptive equation (16) requires steady-state upper and lower bounds z_{nu} and z_{nl}, and their confidence levels λ_{xn} and λ_{yn} respectively. Also, $\hat{z}_n(t) > 0$, z_{nu}, z_{nl}, λ_{xn}, $\lambda_{yn} > 0$ and $\hat{z}_n(t)$, z_{nu}, z_{nl}, λ_{xn}, $\lambda_{yn} \in \mathbb{R}$. The upper and lower bounds z_{nu} and z_{nl} are constants which represent the limits within which $\hat{z}_n(t)$ is desired to settle in, as $t \to \infty$. The constants λ_{xn} and λ_{yn} represent a users confidence in their choice of a desired steady state upper bound z_{nu}, and lower bound z_{nl}.

The operational flow of the proposed novel UAS based adaptive methodology to estimate the parameters of a PMDC motor is shown in Fig. 3 and the pseudo-code is outlined in Algorithm 1. The current and speed errors $e_1(t)$, $e_2(t)$ from (8) and (12) are used in (11), (15) to calculate the inputs $u_1(t)$ and $u_2(t)$ respectively, which are used with the UAS based observer defined in (6)–(7). Errors $e_1(t)$, $e_2(t)$ are also used in (16) as per (17) and (18). The parameters of the PMDC motor are estimated by (16), and the current and speed of the PMDC motor model are then estimated by solving (6)–(7) by incorporating the estimated PMDC motor parameters from (16). For a particular PMDC motor, data sheet parameters are used to determine the appropriate steady-state upper bound z_{nu} and lower bound z_{nl} values. Inappropriate selection of upper and lower bounds and their respective confidence levels can deteriorate the accuracy of estimated parameters. Therefore, parameters values from the datasheet, provided by the manufacturer of a DC motor, are chosen to design the steady state values of the upper and lower bounds for each estimated parameter, i.e. z_{nu} and z_{nl}. In the proposed work, the upper and lower bounds of each parameter are set at $z_n^*(1+\phi_1)$ and $z_n^*(1-\phi_2)$, respectively. Here, z_n^* denotes parameters values from the datasheet, and $\phi_1, \in [1,4]$, $\phi_2 \in [0,1]$, can be set as a certain percentage of z_n^*, or simply by user experience or observation. The confidence level values, i.e. λ_{xn} and λ_{yn}, can be chosen around 50 to get reasonable estimates of DC motor parameters, because the estimated parameters are less sensitive to confidence level selection. The upper and lower bounds, and their respective confidence levels can be calibrated manually within a few trials or by using any optimization technique to minimize the motor speed and/or current estimation error. Optimization techniques such as those available via Matlab's *fmincon* function, or genetic algorithms, particle swarm techniques can be explored, and are left for future work. Note that these parameters are time invariant, and thus, do not need to be readjusted provided that the conditions described in Lemma 4.1, Theorem 4.2, and Theorem 4.3 are satisfied during the estimation process. In previous work (Usman et al., 2018), a UAS based optimization strategy that mitigates the effect of upper, lower bounds and their respective confidence levels, is presented for parameters estimation of a Li-ion battery. Further, the strategy in Usman et al. (2018) provides accurate estimates for Li-ion battery parameters with less computational effort compared to an unguided optimization process.

4. Mathematical justification

This section provides mathematical results related to PMDC motor parameters convergence. The following results establish positiveness conditions on the estimated motor parameters. This is essential for the adaptive observer's estimation error to go to zero.

Lemma 4.1. *For $n \in \{1,2,\ldots,6\}$, let $\lambda_{xn}, \lambda_{yn}, z_{nu}$ and z_{nl} be positive real numbers, such that $\hat{z}_1(t) = \hat{L}_a(t)$, $\hat{z}_2(t) = \hat{R}_a(t)$, $\hat{z}_3(t) = \hat{K}_b(t)$, $\hat{z}_4(t) = \hat{J}(t)$, $\hat{z}_5(t) = \hat{b}(t)$, and $\hat{z}_6(t) = \hat{K}_t(t)$.*

- **If** $\hat{z}_n(t_0)$, λ_{xn}, λ_{yn}, z_{nu}, $z_{nl} > 0$, **then** $\hat{z}_n(t) > 0$ for $n = \{1,2,\ldots,6\}$, for all $t > t_0$.
- **If** $\hat{z}_2(t_0) > \hat{z}_1(t_0) > 0$, $\lambda_{x1} + \lambda_{y1} > \lambda_{x2} + \lambda_{y2}$, and $\lambda_{x1} z_{1u} + \lambda_{y1} z_{1l} < \lambda_{x2} z_{2u} + \lambda_{y2} z_{2l}$, **then** $\hat{z}_2(t) > \hat{z}_1(t)$ for all $t > t_0$.
- **If** $\hat{z}_4(t_0) > \hat{z}_5(t_0) > 0$, $\lambda_{x5} + \lambda_{y5} > \lambda_{x4} + \lambda_{y4}$, and $\lambda_{x5} z_{5u} + \lambda_{y5} z_{5l} < \lambda_{x4} z_{4u} + \lambda_{y4} z_{4l}$, **then** $\hat{z}_4(t) > \hat{z}_5(t)$ for all $t > t_0$.

Proof. Suppose the assumptions stated in Lemma 4.1 hold. Observe that (16) is a stable linear time invariant (LTI) system with $e^2(t) + \lambda_{xn} z_{nu} + \lambda_{yn} z_{nl}$ as an input, then by properties of the convolution integral, the solution of $\hat{z}_n(t)$ can be obtained as

$$\hat{z}_n(t) = \hat{z}_n(t_0) e^{-(\lambda_{xn}+\lambda_{yn})t} + \int_{t_0}^{t} e^2(t-\tau) e^{-(\lambda_{xn}+\lambda_{yn})\tau} d\tau + (\lambda_{xn} z_{nu} + \lambda_{yn} z_{nl}) \int_{t_0}^{t} e^{-(\lambda_{xn}+\lambda_{yn})\tau} d\tau. \tag{19}$$

Because $\hat{z}_n(t_0)$, λ_{xn}, λ_{yn}, z_{nu}, $z_{nl} > 0$ for $n = \{1,2,\ldots,6\}$, and because $e^2(t-\tau) > 0$ for all t, then (19) yields $\hat{z}_n(t) > 0$ for $n = \{1,2,\ldots,6\}$, for all $t > t_0$. This completes the proof of the first statement. As for the proof of the second statement, by the assumptions it is known that $\hat{z}_2(t_0) > \hat{z}_1(t_0) > 0$ and $\lambda_{x1} + \lambda_{y1} > \lambda_{x2} + \lambda_{y2} > 0$. So because of the properties of the exponential function,

$$\hat{z}_1(t_0) e^{-(\lambda_{x1}+\lambda_{y1})t} < \hat{z}_1(t_0) e^{-(\lambda_{x2}+\lambda_{y2})t}, \text{ and}$$
$$\hat{z}_1(t_0) e^{-(\lambda_{x2}+\lambda_{y2})t} < \hat{z}_2(t_0) e^{-(\lambda_{x2}+\lambda_{y2})t}. \tag{20}$$

Further utilizing properties of the exponential function, it is possible to get

$$\int_{t_0}^{t} e^{-(\lambda_{x1}+\lambda_{y1})\tau} d\tau < \int_{t_0}^{t} e^{-(\lambda_{x2}+\lambda_{y2})\tau} d\tau. \tag{21}$$

Now by the assumption that for all $n \in \{1,2,\ldots,6\}$ the constants $\lambda_{xn}, \lambda_{yn}, z_{nu}, z_{nl} > 0$ and $\lambda_{x1} z_{1u} + \lambda_{y1} z_{1l} < \lambda_{x2} z_{2u} + \lambda_{y2} z_{2l}$, and (21) gives

$$(\lambda_{x1} z_{1u} + \lambda_{y1} z_{1l}) \int_{t_0}^{t} e^{-(\lambda_{x1}+\lambda_{y1})\tau} d\tau < (\lambda_{x1} z_{1u} + \lambda_{y1} z_{1l}) \int_{t_0}^{t} e^{-(\lambda_{x2}+\lambda_{y2})\tau} d\tau, \tag{22}$$

and also

$$(\lambda_{x1} z_{1u} + \lambda_{y1} z_{1l}) \int_{t_0}^{t} e^{-(\lambda_{x2}+\lambda_{y2})\tau} d\tau < (\lambda_{x2} z_{2u} + \lambda_{y2} z_{2l}) \int_{t_0}^{t} e^{-(\lambda_{x2}+\lambda_{y2})\tau} d\tau. \tag{23}$$

Algorithm 1 Adaptive Parameters Estimation of a PMDC motor

Requirements: Input voltage $E(t)$, current $i_a(t)$ and speed $\omega(t)$ of a PMDC motor.
Data: Initial time $t = t_0$, step size t_{step} and end time t_{end}. Initialize the iterator variable $k = 1$. Set initial values $\hat{z}_n(t_0)$, upper bounds $\hat{z}_{nu}$ and lower bounds $\hat{z}_{nl}$, and their respective confidence levels λ_{xn} and λ_{yn} for each parameter, where $n \in \{1, \cdots, 6\}$ and $\hat{z}_1(t) = \hat{L}_a(t)$, $\hat{z}_2(t) = \hat{R}_a(t)$, $\hat{z}_3(t) = \hat{K}_b(t)$, $\hat{z}_4(t) = \hat{J}(t)$, $\hat{z}_5(t) = \hat{b}(t)$, and $\hat{z}_6(t) = \hat{K}_t(t)$. Small positive numbers ϵ_1, ϵ_2, ϵ_3, ϵ_4
Output: Estimated PMDC motor parameters $\hat{L}_a, \hat{R}_a, \hat{K}_b, \hat{J}, \hat{b}$ and $\hat{K}_t$.

for $t = t_0 : t_{step} : t_{end}$ **do**
  Read the voltage $E(t)$, current $i_a(t)$, and speed $\omega(t)$ of a PMDC motor.
  Find the current and speed estimation error $e_1(t)$ and $e_2(t)$ using (8) and (12).
  Calculate $u_1(t)$ and $u_2(t)$ from (11) and (15)
  Estimate PMDC motor parameters by using equation (16).
  Solve high gain adaptive estimator equations (6)-(7) to find $\hat{i}_a(t)$ and $\hat{\omega}(t)$.
  Update the current and speed estimation error $e_1(t)$ and $e_2(t)$ using (8) and (12).
  if $\left((|e_1(t)| < \epsilon_1)$ **and** $(|e_2(t)| < \epsilon_2)$ **and** $(|\omega(t)| < \epsilon_3)$ **and** $(|i_a(t)| < \epsilon_4)\right)$ **then**
    $X_1[k] \leftarrow \hat{z}_1(t)$, $X_2[k] \leftarrow \hat{z}_2(t)$, $X_3[k] \leftarrow \hat{z}_3(t)$, $X_4[k] \leftarrow \hat{z}_4(t)$, $X_5[k] \leftarrow \hat{z}_5(t)$ and $X_6[k] \leftarrow \hat{z}_6(t)$.
    $k \leftarrow (k + 1)$.
  else
    Continue loop execution.
  end if
end for
Find the mean value of elements in each array $X_1, \cdots, X_6$ to get the estimates of PMDC motor parameters $\hat{L}_a, \hat{R}_a, \hat{K}_b, \hat{J}, \hat{b}$ and $\hat{K}_t$ respectively.

The required statement for the second result involves $z_1(t)$, and $z_2(t)$, so consider (16) with values of $n \in \{1, 2, 3\}$. Thus (17) provides $e(t) = e_1(t)$. Furthermore, because $e_1^2(t - \tau) > 0$ for all t and by assumptions $\lambda_{x1} + \lambda_{y1} > \lambda_{x2} + \lambda_{y2} > 0$ so,

$$\int_{t_0}^{t} e_1^2(t-\tau)e^{-(\lambda_{x1}+\lambda_{y1})\tau}d\tau < \int_{t_0}^{t} e_1^2(t-\tau)e^{-(\lambda_{x2}+\lambda_{y2})\tau}d\tau. \tag{24}$$

Thus using (20), (22), (23), (24), and the statement of the first result in (19) with $n \in \{1, 2\}$ gives the second result i.e.

$$\hat{z}_2(t) > \hat{z}_1(t) > 0, \text{ for all } t > t_0. \tag{25}$$

Similarly for the proof of the third statement, $e_1(t)$ is replaced by $e_2(t)$. The variables $\hat{z}_1(t_0)$, $\hat{z}_1(t)$, z_{1u}, z_{1l}, λ_{x1}, and λ_{y1} are replaced by $\hat{z}_5(t_0)$, $\hat{z}_5(t)$, z_{5u}, z_{5l}, λ_{x5}, and λ_{y5} respectively. The variables $\hat{z}_2(t_0)$, $\hat{z}_2(t)$, z_{2u}, z_{2l}, λ_{x2}, and λ_{y2} are replaced by $\hat{z}_4(t_0)$, $\hat{z}_4(t)$, z_{4u}, z_{4l}, λ_{x4}, and λ_{y4} respectively. Then following the above process to achieve the proof for the second statement gives $\hat{z}_4(t) > \hat{z}_5(t) > 0$, for all $t > t_0$. This completes the proof. □

Remark 1. By notation, $\hat{z}_2(t) = \hat{R}_a(t)$, $\hat{z}_1(t) = \hat{L}_a(t)$, $\hat{z}_4(t) = \hat{J}(t)$, and $\hat{z}_5(t) = \hat{b}(t)$. From the results shown above in Lemma 4.1, it is established that as long as the conditions needed for Lemma 4.1 to hold are satisfied, then, $\frac{\hat{R}_a(t)}{\hat{L}_a(t)} > 1$, and $\frac{\hat{b}(t)}{\hat{J}(t)} < 1$, for all $t > t_0$.

Using the results established above, the following theorem shows that some estimated motor parameters converge to their actual values when using the proposed adaptive observer. Following this, an analysis of estimation accuracy leads to the conclusion that the proposed method allows all motor parameters to be estimated. Theorem 4.2 provides justification for convergence of parameters described in (1), i.e. $\hat{L}_a(t) \to L_a$, $\hat{R}_a(t) \to R_a$ and $\hat{K}_b(t) \to K_b$ as $t \to \infty$. The estimation process of these parameters is carried out by utilizing the UAS based high-gain adaptive estimator presented in (6). Further, Theorem 4.2 requires knowing the actual DC motor input voltage $E(t)$ and actual DC motor speed $\omega(t)$, and the proof is based on the motor current estimation error $e_1(t)$. Whereas, Theorem 4.3 provides mathematical justification for convergence of the parameters described in (2), i.e. $b(t)$, $J(t)$, and K_t, using the UAS based adaptive estimator given in (7). In contrast to Theorem 4.2, the results in Theorem 4.3 show $\frac{\hat{b}(t)}{\hat{J}(t)} \to \frac{b}{J}$, and $\frac{\hat{K}_t(t)}{\hat{J}(t)} \to \frac{K_t}{J}$ as $t \to \infty$. Moreover, Theorem 4.3 requires knowing the actual DC motor input current $i(t)$, actual DC motor speed $\omega(t)$, and the result is based on the motor speed estimation error $e_2(t)$.

Theorem 4.2. *Suppose the PMDC motor operates at no load condition with input voltage $E(t) > 0$, and let $i_a(t), \omega(t) \in \mathbb{R}$ represent the motor armature current, and motor speed respectively. Let time $t \geq t_0$, $t \in \mathbb{R}$, Further, suppose $E(t) \to 0$, as $t \to \infty$, $E(t) \neq 0$; $i_a(t) \to 0$, as $t \to \infty$, $i_a(t) \neq 0$, $\frac{di_a(t)}{dt} \to 0$ as $t \to \infty$; and $\omega(t) \to 0$ as $t \to \infty$, $\omega(t) \neq 0$. **If** all conditions needed for Lemma 4.1 to hold are satisfied, **then** $\hat{L}_a(t) \to L_a$, $\hat{R}_a(t) \to R_a$ and $\hat{K}_b(t) \to K_b$, as $t \to \infty$.*

Proof. Suppose the assumptions stated above are satisfied. Considering the time derivative of (8), and using (6) gives

$$\dot{e}_1(t) = \frac{di_a(t)}{dt} - \frac{E(t)}{\hat{L}_a(t)} + \frac{\hat{R}_a(t)\hat{i}_a(t)}{\hat{L}_a(t)} + \frac{\hat{K}_b(t)\omega(t)}{\hat{L}_a(t)} - u_1(t). \tag{26}$$

Multiply (26) by $\frac{\hat{L}_a(t)}{\hat{R}_a(t)}$, where $\hat{L}_a(t) \neq 0$, and $\hat{R}_a(t) \neq 0$ as proven in Lemma 4.1, to get the following.

$$\frac{\hat{L}_a(t)}{\hat{R}_a(t)}\dot{e}_1(t) = \frac{\hat{L}_a(t)}{\hat{R}_a(t)}\frac{di_a(t)}{dt} - \frac{E(t)}{\hat{R}_a(t)} + \hat{i}_a(t) + \frac{\hat{K}_b(t)\omega(t)}{\hat{R}_a(t)} - \frac{\hat{L}_a(t)}{\hat{R}_a(t)}u_1(t) \tag{27}$$

Now subtracting and adding $\frac{\hat{R}_a(t)}{\hat{L}_a(t)}e_1(t)$ to the R.H.S of (27), and further realizing that using the definition of $e_1(t)$ from (8) with $-\frac{\hat{R}_a(t)}{\hat{L}_a(t)}e_1(t) + \frac{\hat{R}_a(t)}{\hat{L}_a(t)}e_1(t)$ gives $-\frac{\hat{R}_a(t)}{\hat{L}_a(t)}e_1(t) + \frac{\hat{R}_a(t)}{\hat{L}_a(t)}i_a(t) - \frac{\hat{R}_a(t)}{\hat{L}_a(t)}\hat{i}_a(t)$. So the result of subtracting and adding $\frac{\hat{R}_a(t)}{\hat{L}_a(t)}e_1(t)$ to the R.H.S of (27), and grouping terms with $\hat{i}_a(t)$ together can be written as,

$$\begin{aligned}\frac{\hat{L}_a(t)}{\hat{R}_a(t)}\dot{e}_1(t) = {} & \frac{\hat{L}_a(t)}{\hat{R}_a(t)}\frac{di_a(t)}{dt} - \frac{E(t)}{\hat{R}_a(t)} + \hat{i}_a(t)\left(1 - \frac{\hat{R}_a(t)}{\hat{L}_a(t)}\right) \\ & + \frac{\hat{K}_b(t)\omega(t)}{\hat{R}_a(t)} - \frac{\hat{L}_a(t)}{\hat{R}_a(t)}u_1(t) - \frac{\hat{R}_a(t)}{\hat{L}_a(t)}e_1(t) + \frac{\hat{R}_a(t)}{\hat{L}_a(t)}i_a(t).\end{aligned} \tag{28}$$

Because the conditions of Lemma 4.1 are satisfied so $\frac{\hat{R}_a(t)}{\hat{L}_a(t)} > 1$, $\hat{L}_a(t) > 0$, for all $t \geq t_0$. Also $\hat{i}_a(t) \geq 0$ for all $t \geq t_0$ from (6), thus

$$\hat{i}_a(t)\left(1 - \frac{\hat{R}_a(t)}{\hat{L}_a(t)}\right) \leq 0 \text{ for all } t \geq t_0. \tag{29}$$

Adding $\frac{\hat{L}_a(t)}{\hat{R}_a(t)}\frac{di_a(t)}{dt} - \frac{E(t)}{\hat{R}_a(t)} + \frac{\hat{K}_b(t)\omega(t)}{\hat{R}_a(t)} - \frac{\hat{L}_a(t)}{\hat{R}_a(t)}u_1(t) - \frac{\hat{R}_a(t)}{\hat{L}_a(t)}e_1(t) + \frac{\hat{R}_a(t)}{\hat{L}_a(t)}i_a(t)$ to both sides of (29), then using (28), and thereafter multiplying by $\frac{\hat{R}_a(t)}{\hat{L}_a(t)}$, and recalling from above that $\frac{\hat{R}_a(t)}{\hat{L}_a(t)} > 1$, $\hat{L}_a(t) > 0$, for all $t \geq t_0$, results in the following,

$$\dot{e}_1(t) \leq \frac{di_a(t)}{dt} + \left(\frac{\hat{R}_a(t)}{\hat{L}_a(t)}\right)^2 i_a(t) - \frac{E(t)}{\hat{L}_a(t)} + \frac{\hat{K}_b(t)\omega(t)}{\hat{L}_a(t)} - u_1(t) - \left(\frac{\hat{R}_a(t)}{\hat{L}_a(t)}\right)^2 e_1(t). \tag{30}$$

Now let

$$\delta_1(t) = \frac{di_a(t)}{dt} + \left(\frac{\hat{R}_a(t)}{\hat{L}_a(t)}\right)^2 i_a(t), \text{ and} \tag{31}$$

$$\delta_2(t) = i_a(t) + \frac{di_a(t)}{dt}. \tag{32}$$

Also, because $\left(\frac{E(t)}{\hat{L}_a(t)} + e_1(t)\right)^2 \geq 0$ for all $t \geq t_0$, i.e. so $\frac{1}{2}\left(\frac{E(t)}{\hat{L}_a(t)}\right)^2 + \frac{1}{2}e_1^2(t) + \frac{E(t)e_1(t)}{\hat{L}_a(t)} \geq 0$. Similarly, $\left(\frac{\hat{K}_b(t)\omega(t)}{\hat{L}_a(t)} - e_1(t)\right)^2 \geq 0$, i.e. $\frac{1}{2}\left(\frac{\hat{K}_b(t)\omega(t)}{\hat{L}_a(t)}\right)^2 + \frac{1}{2}e_1^2(t) - \frac{\hat{K}_b(t)\omega(t)e_1(t)}{\hat{L}_a(t)} \geq 0$. Therefore for all $t \geq t_0$

$$0 \leq \left(\frac{1}{2}\left(\frac{E(t)}{\hat{L}_a(t)}\right)^2 + \frac{1}{2}e_1^2(t) + \frac{E(t)e_1(t)}{\hat{L}_a(t)} + \frac{1}{2}\left(\frac{\hat{K}_b(t)\omega(t)}{\hat{L}_a(t)}\right)^2 + \frac{1}{2}e_1^2(t) - \frac{\hat{K}_b(t)\omega(t)e_1(t)}{\hat{L}_a(t)}\right). \tag{33}$$

Re-arranging the above gives

$$\left(\frac{1}{2}\left(\frac{E(t)}{\hat{L}_a(t)}\right)^2 + \frac{1}{2}\left(\frac{\hat{K}_b(t)\omega(t)}{\hat{L}_a(t)}\right)^2 + e_1^2(t)\right) \geq \left(-\frac{E(t)e_1(t)}{\hat{L}_a(t)} + \frac{\hat{K}_b(t)\omega(t)e_1(t)}{\hat{L}_a(t)}\right). \tag{34}$$

The above equations have set up terms needed for the rest of the proof below. Further the proof considers two cases, i.e. the error $e_1(t)$ being positive, or negative, and shows that each case produces an equation having a particular form. And this particular form helps show that in both cases, the error $e_1(t)$ converges to zero.

Case. 1. Consider $e_1(t) > 0$, at some time instant $t > t_0$. Then, multiplying (30) by $e_1(t)$, and using the definition of $\delta_1(t)$ from (31) results in

$$e_1(t)\dot{e}_1(t) \leq \delta_1(t)e_1(t) - \frac{E(t)e_1(t)}{\hat{L}_a(t)} + \frac{\hat{K}_b(t)\omega(t)e_1(t)}{\hat{L}_a(t)} - u_1(t)e_1(t) - \left(\frac{\hat{R}_a(t)}{\hat{L}_a(t)}\right)^2 e_1^2(t). \tag{35}$$

Now again as discussed earlier $\left(\hat{R}_a(t)/\hat{L}_a(t)\right) > 1$, and $\hat{L}_a(t) > 0$ for all $t \geq t_0$, then $\left(\hat{R}_a(t)/\hat{L}_a(t)\right)^2 > 1$. Also $e_1^2(t) > 0$ so $\left(\hat{R}_a(t)/\hat{L}_a(t)\right)^2 e_1^2(t) > e_1^2(t)$, or $-\left(\hat{R}_a(t)/\hat{L}_a(t)\right)^2 e_1^2(t) < -e_1^2(t)$. Using this together with (35) results in

$$e_1(t)\dot{e}_1(t) \leq -e_1^2(t) + \delta_1(t)e_1(t) - \frac{E(t)e_1(t)}{\hat{L}_a(t)} + \frac{\hat{K}_b(t)\omega(t)e_1(t)}{\hat{L}_a(t)} - u_1(t)e_1(t). \tag{36}$$

Consider $(e_1(t) - \delta_1(t))^2 \geq 0$, i.e. $\frac{1}{2}e_1^2(t) + \frac{1}{2}\delta_1^2(t) \geq \delta_1(t)e_1(t)$ for all $t \geq t_0$. From this, and substituting (11) in (36) and thereafter using (34) gives us

$$e_1(t)\dot{e}_1(t) \leq \frac{1}{2}e_1^2(t) + \frac{1}{2}\delta_1^2(t) + \frac{1}{2}\left(\frac{E(t)}{\hat{L}_a(t)}\right)^2 + \frac{1}{2}\left(\frac{\hat{K}_b(t)\omega(t)}{\hat{L}_a(t)}\right)^2 - N(k_1(t))e_1^2(t). \tag{37}$$

Because $\frac{d}{dt}\left(\frac{1}{2}e_1^2(t)\right) = e_1(t)\dot{e}_1(t)$, thus integrating (37) from t_0 to t, and using (9) gives

$$\frac{1}{2}e_1^2(t) \leq \frac{1}{2}(k_1(t) - k_1(t_0)) + \frac{1}{2}\int_{t_0}^{t}\delta_1^2(\tau)d\tau + \frac{1}{2}\int_{t_0}^{t}\left(\frac{E(\tau)}{\hat{L}_a(\tau)}\right)^2 d\tau + \frac{1}{2}\int_{t_0}^{t}\left(\frac{\hat{K}_b(\tau)\omega(\tau)}{\hat{L}_a(\tau)}\right)^2 d\tau - \int_{t_0}^{t} N(k_1(\tau))\dot{k}_1(\tau)d\tau. \tag{38}$$

Let $\tilde{k}_1(t) = k_1(t) - k_1(t_0)$. Now dividing (38) by $\tilde{k}_1(t)$, multiplying by two, and recognizing that $\int_{t_0}^{t} N(k_1)\dot{k}_1 dt = \int_{k_1(t_0)}^{k_1(t)} N(\tau)d\tau$ let us write

$$\frac{e_1^2(t)}{\tilde{k}_1(t)} \leq 1 + \frac{1}{\tilde{k}_1(t)}\int_{t_0}^{t}\delta_1^2(\tau)d\tau + \frac{1}{\tilde{k}_1(t)}\int_{t_0}^{t}\left(\frac{E(\tau)}{\hat{L}_a(\tau)}\right)^2 d\tau + \frac{1}{\tilde{k}_1(t)}\int_{t_0}^{t}\left(\frac{\hat{K}_b(\tau)\omega(\tau)}{\hat{L}_a(\tau)}\right)^2 d\tau - \frac{2}{\tilde{k}_1(t)}\int_{k_1(t_0)}^{k_1(t)} N(\tau)d\tau. \tag{39}$$

Eq. (39) is an important point that is revisited at the end of the proof. For now, case 2 below shows that even when the error $e_1(t) < 0$, it is possible to arrive at an equation with a form similar to (39). The strategy of the proof then, is to show that in both cases when the error $e_1(t)$ acquires either negative or positive sign at some time instant say $t^* > t_0$, and supposing that the adaptive gain $k_1(t)$ diverges to infinity as time $t \to \infty$, $t > t^*$, results in a contradiction. Thus, first consider case 2, and generate an equation of the form similar to (39). This is done as shown below.

Case. 2. Now suppose $e_1(t) < 0$, at some time instant $t > t_0$. Considering the time derivative of $e_1(t)$, and then adding and subtracting $e_1(t)$ on R.H.S of $\dot{e}_1(t)$ gives

$$\dot{e}_1(t) = -e_1(t) + e_1(t) + \frac{di_a(t)}{dt} - \frac{d\hat{i}_a(t)}{dt}. \tag{40}$$

Using (8) and (6) in (40) and thereafter using the definition of $\delta_2(t)$ from (32) provides

$$\dot{e}_1(t) = -e_1(t) + \delta_2(t) - \hat{i}_a(t) - \frac{E(t)}{\hat{L}_a(t)} + \frac{\hat{R}_a(t)\hat{i}_a(t)}{\hat{L}_a(t)} + \frac{\hat{K}_b(t)\omega(t)}{\hat{L}_a(t)} - u_1(t). \tag{41}$$

Further multiplying (29) by −1, it is possible to get

$$\frac{\hat{R}_a(t)\hat{i}_a(t)}{\hat{L}_a(t)} - \hat{i}_a(t) \geq 0, \text{ for all } t \geq t_0. \tag{42}$$

Adding $-e_1(t) + \delta_2(t) - u_1(t) - \frac{E(t)}{\hat{L}_a(t)} + \frac{\hat{K}_b(t)\omega(t)}{\hat{L}_a(t)}$ on both sides of (42) and then using (41) on the L.H.S results in

$$\dot{e}_1(t) \geq -e_1(t) + \delta_2(t) - u_1(t) - \frac{E(t)}{\hat{L}_a(t)} + \frac{\hat{K}_b(t)\omega(t)}{\hat{L}_a(t)}. \tag{43}$$

Because in this case $e_1(t) < 0$, thus multiplying (43) by $e_1(t)$ produces

$$e_1(t)\dot{e}_1(t) \leq -e_1^2(t) + \delta_2(t)e_1(t) - u_1(t)e_1(t) - \frac{E(t)e_1(t)}{\hat{L}_a(t)} + \frac{\hat{K}_b(t)\omega(t)e_1(t)}{\hat{L}_a(t)}. \tag{44}$$

Consider $(e_1(t) - \delta_2(t))^2 \geq 0$, i.e. $\frac{1}{2}e_1^2(t) + \frac{1}{2}\delta_2^2(t) \geq \delta_2(t)e_1(t)$ for all $t \geq t_0$. From the above, and substituting (11) in (44) and thereafter using (34) provides

$$e_1(t)\dot{e}_1(t) \leq \frac{1}{2}e_1^2(t) + \frac{1}{2}\delta_2^2(t) + \frac{1}{2}\left(\frac{E(t)}{\hat{L}_a(t)}\right)^2 + \frac{1}{2}\left(\frac{\hat{K}_b(t)\omega(t)}{\hat{L}_a(t)}\right)^2 - N(k_1(t))e_1^2(t). \tag{45}$$

Again, because $\frac{d}{dt}\left(\frac{1}{2}e_1^2(t)\right) = e_1(t)\dot{e}_1(t)$, thus integrating (45) from t_0 to t, and using (9) gives

$$\frac{1}{2}e_1^2(t) \leq \frac{1}{2}(k_1(t) - k_1(t_0)) + \frac{1}{2}\int_{t_0}^{t}\delta_2^2(\tau)d\tau + \frac{1}{2}\int_{t_0}^{t}\left(\frac{E(\tau)}{\hat{L}_a(\tau)}\right)^2 d\tau + \frac{1}{2}\int_{t_0}^{t}\left(\frac{\hat{K}_b(\tau)\omega(\tau)}{\hat{L}_a(\tau)}\right)^2 d\tau - \int_{t_0}^{t} N(k_1(\tau))\dot{k}_1(\tau)d\tau \tag{46}$$

And again just as in Case 1, letting $\tilde{k}_1(t) = k_1(t) - k_1(t_0)$, now dividing (46) by $\tilde{k}_1(t)$, multiplying by two, and recognizing that $\int_{t_0}^{t} N(k_1)\dot{k}_1 dt = \int_{k_1(t_0)}^{k_1(t)} N(\tau)d\tau$ gives us

$$\frac{e_1^2(t)}{\tilde{k}_1(t)} \leq 1 + \frac{1}{\tilde{k}_1(t)}\int_{t_0}^{t}\delta_2^2(\tau)d\tau + \frac{1}{\tilde{k}_1(t)}\int_{t_0}^{t}\left(\frac{E(\tau)}{\hat{L}_a(\tau)}\right)^2 d\tau$$

$$+\frac{1}{\widetilde{k}_1(t)}\int_{t_0}^{t}\left(\frac{\hat{K}_b(\tau)\omega(\tau)}{\hat{L}_a(\tau)}\right)^2 d\tau-\frac{2}{\widetilde{k}_1(t)}\int_{k_1(t_0)}^{k_1(t)}N(\tau)d\tau. \tag{47}$$

Notice now that the form of (47) is very similar to the form of (39). The only difference between the two equations is that the second term on the R.H.S. of (47) is $\frac{1}{\widetilde{k}_1(t)}\int_{t_0}^{t}\delta_2^2(\tau)d\tau$, where as the second term on the R.H.S. of (39) is $\frac{1}{\widetilde{k}_1(t)}\int_{t_0}^{t}\delta_1^2(\tau)d\tau$. First, consider the term $\delta_1(t)$, which from (31), can be rewritten as $\delta_1(t)=\frac{di_a(t)}{dt}+\left(i_a(t)/\left(\frac{\hat{L}_a(t)}{\hat{R}_a(t)}\right)^2\right)$. Now from Lemma 4.1, and Remark 1 it is known that $0<\left(\hat{L}_a(t)/\hat{R}_a(t)\right)<1$, for all $t>t_0$. Also by the assumptions of this theorem it is known that $i_a(t)\to 0$ as $t\to\infty$, $i_a(t)\neq 0$, $\frac{di_a(t)}{dt}\to 0$. This means that $\delta_1(t)\to 0$ as $t\to\infty$. Also, from (32), and the above stated assumptions of this theorem, $\delta_2(t)\to 0$ as $t\to\infty$. Further, by assumptions $E(t)\to 0$, as $t\to\infty$, $E(t)\neq 0$, and from Lemma 4.1 it is known that $\hat{L}_a(t)>0$, for all $t>t_0$. This means that $\left(E(t)/\hat{L}_a(t)\right)\to 0$, as $t\to\infty$. Now notice that $\left(\hat{K}_b(t)\omega(t)/\hat{L}_a(t)\right)=\left(\omega(t)/\left(\frac{\hat{L}_a(t)}{\hat{K}_b(t)}\right)\right)$. However, by Lemma 4.1, both $\hat{L}_a(t)$, and $\hat{K}_b(t)$ are positive for all time. Thus, $\left(\hat{L}_a(t)/\hat{K}_b(t)\right)>0$ for all $t>t_0$, and by assumptions $\omega(t)\to 0$ as $t\to\infty$, $\omega(t)\neq 0$. This shows that $\left(\hat{K}_b(t)\omega(t)/\hat{L}_a(t)\right)\to 0$ as $t\to\infty$.

Thus, from the above paragraph it is possible to conclude that the terms $\int_{t_0}^{t}\delta_1^2(\tau)d\tau$, $\int_{t_0}^{t}\delta_2^2(\tau)d\tau$, $\int_{t_0}^{t}\left(\frac{E(\tau)}{\hat{L}_a(\tau)}\right)^2 d\tau$, and $\int_{t_0}^{t}\left(\frac{\hat{K}_b(\tau)\omega(\tau)}{\hat{L}_a(\tau)}\right)^2 d\tau$ in (39) and (47), are bounded. Now suppose that at some instant of time $t^*>t_0$, the error $e_1(t)$ is either positive or negative, and further suppose that as $t\to\infty$, $t>t^*$, then $k_1(t)\to\infty$. From the above discussion, and observing the R.H.S. of (39), (47) shows that the first four terms on the R.H.S. of (39), (47) are bounded. Also the L.H.S. of (39), (47) are both positive. So if $k_1(t)\to\infty$ as $t\to\infty$, $t>t^*$ then according to (4), the Nussbaum function i.e. the fifth term on the R.H.S. of (39), (47) can take values at $+\infty$, which violates the positiveness of the L.H.S of (39), and (47). Thus $k_1(t)$ does not go to infinity with time, but from (9) it is seen that $k_1(t)$ is an increasing function. So, from this it can be concluded that $k_1(t)$ is bounded, i.e $k_1(t)\to k_{1\infty}$ as $t\to\infty$, regardless of whether the error $e_1(t)$ is negative or positive at some time instant $t^*>t_0$. This implies that as $t\to\infty$, $\dot{k}_1(t)\to 0$ i.e. $e_1^2(t)\to 0$, or $e_1(t)\to 0$. Using (11), because $e_1(t)\to 0$, and from Gorenflo and Mainardi (1996) and Li and Chen (2009) it is known that $N(k_1(t))$ approaches some constant value as $k_1(t)\to k_{1\infty}$, this leads to $u_1(t)\to 0$. And therefore, by (8) it is possible to get $\hat{i}_a(t)\to i_a(t)$. This further gives $\frac{d\hat{i}_a(t)}{dt}\to\frac{di_a(t)}{dt}$ as $t\to\infty$. And so, using (1) and (6), it is possible to now write

$$\frac{E(t)}{L_a}-\frac{R_a}{L_a}i_a(t)-\frac{K_b}{L_a}\omega=\frac{E(t)}{\hat{L}_a(t)}-\frac{\hat{R}_a(t)}{\hat{L}_a(t)}i_a(t)-\frac{\hat{K}_b(t)}{\hat{L}_a(t)}\omega(t), \tag{48}$$

which can be re-arranged to get the following,

$$\begin{bmatrix}\frac{R_a}{L_a}-\frac{\hat{R}_a(t)}{\hat{L}_a(t)} & \frac{K_b}{L_a}-\frac{\hat{K}_b(t)}{\hat{L}_a(t)}\end{bmatrix}\begin{bmatrix}i_a(t)\\ \omega(t)\end{bmatrix}=\left(\frac{1}{L_a}-\frac{1}{\hat{L}_a(t)}\right)E(t). \tag{49}$$

By assumptions, $\omega(t)\to 0$, $i_a(t)\to 0$ as $t\to\infty$, and $E(t)\neq 0$. Therefore from (49) the following is obtained,

$$\left(\frac{1}{L_a}-\frac{1}{\hat{L}_a(t)}\right)E(t)\to 0,\ \text{as } t\to\infty. \tag{50}$$

And because $E(t)\neq 0$, this leads to $\hat{L}_a(t)\to L_a$, as $t\to\infty$. Thus, using the above with (49) provides

$$\begin{bmatrix}\left(\frac{R_a}{L_a}-\frac{\hat{R}_a(t)}{L_a}\right) & \left(\frac{K_b}{L_a}-\frac{\hat{K}_b(t)}{L_a}\right)\end{bmatrix}\begin{bmatrix}i_a(t)\\ \omega(t)\end{bmatrix}=0 \tag{51}$$

Further because $i_a(t)\neq 0$, and $\omega(t)\neq 0$, then from (51), $\hat{R}_a(t)\to R_a$ and $\hat{K}_b(t)\to K_b$ as $t\to\infty$. Thus proving the required results, and completing this theorem. □

The above results show convergence of some of the DC motor's estimated parameters to the actual values. The following result provides a proof related to the remaining DC motor parameters.

Theorem 4.3. *Suppose the PMDC motor operates at no load condition with input voltage $E(t)>0$. Let time $t\geq t_0$, $t\in\mathbb{R}$. Further let $i_a(t),\omega(t)\in\mathbb{R}$ be the motor armature current, and speed respectively. Suppose $\omega(t)\to 0$ as $t\to\infty$, $\omega(t)\neq 0$, $\dot{\omega}(t)\to 0$, as $t\to\infty$; and $i_a(t)\to 0$ as $t\to\infty$, $i_a(t)\neq 0$. **If** all conditions required for Lemma 4.1 to hold are satisfied, **then** $\frac{\hat{b}(t)}{\hat{J}(t)}\to\frac{b}{J}$, and $\frac{\hat{K}_t(t)}{\hat{J}(t)}\to\frac{K_t}{J}$, as $t\to\infty$.*

Proof. Suppose the assumptions mentioned are satisfied. Taking the time derivative of (12), then adding and subtracting $e_2(t)$ to the R.H.S, and thereafter using (12) provides

$$\dot{e}_2(t)=-e_2(t)-\dot{\hat{\omega}}(t)-\hat{\omega}(t)+(\omega(t)+\dot{\omega}(t)). \tag{52}$$

Further, let

$$\delta_3(t)=\omega(t)+\dot{\omega}(t),\ \text{and} \tag{53}$$

$$\delta_4(t)=\dot{\omega}(t)-\omega(t). \tag{54}$$

Reorganizing (52) using (53), and (7) results in the following

$$\dot{e}_2(t)=-e_2(t)-\frac{\hat{K}_t(t)i_a(t)}{\hat{J}(t)}+\frac{\hat{b}(t)\hat{\omega}(t)}{\hat{J}(t)}-u_2(t)-\hat{\omega}(t)+\delta_3(t). \tag{55}$$

By Lemma 4.1, and Remark 1, it is known that $\frac{\hat{b}(t)}{\hat{J}(t)}<1$ for all $t\geq t_0$, and from (7)$\hat{\omega}(t)\geq 0$ for all $t\geq t_0$. From this, one can write $\frac{\hat{b}(t)\hat{\omega}(t)}{\hat{J}(t)}\leq\hat{\omega}(t)$, or equivalently

$$\frac{\hat{b}(t)\hat{\omega}(t)}{\hat{J}(t)}-\hat{\omega}(t)\leq 0\ \text{for all } t\geq t_0. \tag{56}$$

By adding $-e_2(t)-u_2(t)+\delta_3(t)-\frac{\hat{K}_t(t)i_a(t)}{\hat{J}(t)}$ to both sides of (56),

$$\left(-e_2(t)-u_2(t)+\delta_3(t)-\frac{\hat{K}_t(t)i_a(t)}{\hat{J}(t)}+\frac{\hat{b}(t)\hat{\omega}(t)}{\hat{J}(t)}-\hat{\omega}(t)\right)\leq\left(-e_2(t)-u_2(t)+\delta_3(t)-\frac{\hat{K}_t(t)i_a(t)}{\hat{J}(t)}\right), \tag{57}$$

and then substitution of (55) on the L.H.S of (57) gives

$$\dot{e}_2(t)\leq-e_2(t)-u_2(t)+\delta_3(t)-\frac{\hat{K}_t(t)i_a(t)}{\hat{J}(t)}. \tag{58}$$

Also, $\left(\frac{\hat{K}_t(t)i_a(t)}{\hat{J}(t)}+e_2(t)\right)^2\geq 0$ for all $t\geq t_0$, i.e.

$$\frac{1}{2}\left(\frac{\hat{K}_t(t)i_a(t)}{\hat{J}(t)}\right)^2+\frac{1}{2}e_2^2(t)\geq-\frac{\hat{K}_t(t)i_a(t)e_2(t)}{\hat{J}(t)}. \tag{59}$$

At this point the basic equations or terms on which the rest of the proof depends, are available. Further, just like in Theorem 4.2, consider two cases. The first case is where $e_2(t)$ is positive at some time instant $t^*>t_0$, and the second case is where $e_2(t)$ is negative at some time instant $t^*>t_0$. As before, it is now shown that both these cases result in two equations which have similar forms, and this form leads to the result that the error $e_2(t)$ converges to zero as time goes to infinity.

Case. 1. Suppose $e_2(t)>0$ at some time instant $t\geq t_0$, then from (58)

$$e_2(t)\dot{e}_2(t)\leq-e_2^2(t)-e_2(t)u_2(t)+e_2(t)\delta_3(t)-\frac{\hat{K}_t(t)i_a(t)e_2(t)}{\hat{J}(t)}. \tag{60}$$

Now considering $(e_2(t)-\delta_3(t))^2\geq 0$ gives us $\frac{1}{2}e_2^2(t)+\frac{1}{2}\delta_3^2(t)\geq e_2(t)\delta_3(t)$ for all $t\geq t_0$. Using this and (59), and then substituting (15) in (60) provides us the following,

$$e_2(t)\dot{e}_2(t)\leq\frac{1}{2}\delta_3^2(t)-N(k_2(t))e_2^2(t)+\frac{1}{2}\left(\frac{\hat{K}_t(t)i_a(t)}{\hat{J}(t)}\right)^2. \tag{61}$$

Because $\frac{d}{dt}\left(\frac{1}{2}e_2^2(t)\right) = e_2(t)\dot{e}_2(t)$, thus integrating (61) from t_0 to t, and using (13) gives us

$$\frac{1}{2}e_2^2(t) \le \frac{1}{2}\int_{t_0}^{t}\delta_3^2(\tau)d\tau - \int_{t_0}^{t}N(k_2(\tau))\dot{k}_2(\tau)d\tau + \frac{1}{2}\int_{t_0}^{t}\left(\frac{\hat{K}_t(\tau)i_a(\tau)}{\hat{J}(\tau)}\right)^2 d\tau. \tag{62}$$

Now let $\widetilde{k}_2(t) = k_2(t) - k_2(t_0)$, then dividing (62) by $\widetilde{k}_2(t)$ and recognizing that $\int_{t_0}^{t}N(k_2)\dot{k}_2 dt = \int_{k_2(t_0)}^{k_2(t)}N(\tau)d\tau$ provides

$$\frac{e_2^2(t)}{2\widetilde{k}_2(t)} \le \frac{1}{2\widetilde{k}_2(t)}\int_{t_0}^{t}\delta_3^2(\tau)d\tau - \frac{1}{\widetilde{k}_2(t)}\int_{k_2(t_0)}^{k_2(t)}N(\tau)d\tau + \frac{1}{2\widetilde{k}_2(t)}\int_{t_0}^{t}\left(\frac{\hat{K}_t(\tau)i_a(\tau)}{\hat{J}(\tau)}\right)^2 d\tau. \tag{63}$$

Eq. (63) is an important point in this proof, and discussion returns to (63) further in the proof. As mentioned earlier, consider the case of negative error $e_2(\cdot)$, and develop an equation which has a form similar to (63).

Case. 2. Now suppose that $e_2(t) < 0$ at some time instant $t \ge t_0$. Taking the time derivative of (12), then adding and subtracting $e_2(t)$ to the R.H.S, and thereafter using (12) and re-arranging terms gives

$$\dot{e}_2(t) = e_2(t) - \dot{\hat{\omega}}(t) + \hat{\omega}(t) + (\dot{\omega}(t) - \omega(t)). \tag{64}$$

Reorganize (64), using (54) and (7) to get

$$\dot{e}_2(t) = e_2(t) - \frac{\hat{K}_t(t)i_a(t)}{\hat{J}(t)} + \frac{\hat{b}(t)\hat{\omega}(t)}{\hat{J}(t)} - u_2(t) + \hat{\omega}(t) + \delta_4(t). \tag{65}$$

From Lemma 4.1, $\frac{\hat{b}(t)}{\hat{J}(t)} > 0$ for all $t \ge t_0$, and from (7), $\hat{\omega}(t) > 0$ for all $t \ge 0$, thus

$$\frac{\hat{b}(t)\hat{\omega}(t)}{\hat{J}(t)} + \hat{\omega}(t) \ge 0 \text{ for all } t \ge t_0. \tag{66}$$

Adding $e_2(t) - u_2(t) + \delta_4(t) - \frac{\hat{K}_t(t)i_a(t)}{\hat{J}(t)}$ on both sides of (66) gives

$$\left(e_2(t) - u_2(t) + \delta_4(t) - \frac{\hat{K}_t(t)i_a(t)}{\hat{J}(t)} + \frac{\hat{b}(t)\hat{\omega}(t)}{\hat{J}(t)} + \hat{\omega}(t)\right) \ge \left(e_2(t) - u_2(t) + \delta_4(t) - \frac{\hat{K}_t(t)i_a(t)}{\hat{J}(t)}\right), \tag{67}$$

Using (65) in (67) and then multiplying with $e_2(t)$, where $e_2(t) < 0$ in this case, gives

$$e_2(t)\dot{e}_2(t) \le e_2^2(t) - e_2(t)u_2(t) + e_2(t)\delta_4(t) - \frac{\hat{K}_t(t)i_a(t)e_2(t)}{\hat{J}(t)}. \tag{68}$$

Consider $(e_2(t) - \delta_4(t))^2 \ge 0$, i.e. $\frac{1}{2}e_2^2(t) + \frac{1}{2}\delta_4^2(t) \ge e_2(t)\delta_4(t)$ for all $t \ge t_0$. Using the above and (59), and substituting (15) in (68) gives

$$e_2(t)\dot{e}_2(t) \le 2e_2^2(t) + \frac{1}{2}\delta_4^2(t) - N(k_2(t))e_2^2(t) + \frac{1}{2}\left(\frac{\hat{K}_t(t)i_a(t)}{\hat{J}(t)}\right)^2. \tag{69}$$

Because $\frac{d}{dt}\left(\frac{1}{2}e_2^2(t)\right) = e_2(t)\dot{e}_2(t)$, thus integrating (69) from t_0 to t, and using (13) gives

$$\frac{1}{2}e_2^2(t) \le 2(k_2(t) - k_2(t_0)) + \frac{1}{2}\int_{t_0}^{t}\delta_4^2(\tau)d\tau - \int_{t_0}^{t}N(k_2(\tau))\dot{k}_2(\tau)d\tau + \frac{1}{2}\int_{t_0}^{t}\left(\frac{\hat{K}_t(\tau)i_a(\tau)}{\hat{J}(\tau)}\right)^2 d\tau. \tag{70}$$

Now letting $\widetilde{k}_2(t) = k_2(t) - k_2(t_0)$, dividing (70) by $\widetilde{k}_2(t)$, and again recognizing that $\int_{t_0}^{t}N(k_2)\dot{k}_2 dt = \int_{k_2(t_0)}^{k_2(t)}N(\tau)d\tau$ provides

$$\frac{e_2^2(t)}{2\widetilde{k}_2(t)} \le 2 + \frac{1}{2\widetilde{k}_2(t)}\int_{t_0}^{t}\delta_4^2(\tau)d\tau - \frac{1}{\widetilde{k}_2(t)}\int_{k_2(t_0)}^{k_2(t)}N(\tau)d\tau + \frac{1}{2\widetilde{k}_2(t)}\int_{t_0}^{t}\left(\frac{\hat{K}_t(\tau)i_a(\tau)}{\hat{J}(\tau)}\right)^2 d\tau. \tag{71}$$

Now notice that (71) and (63) are similar in form, the only major difference between (63) and (71) is that, (71) also has a constant term on the R.H.S. By assumptions $\omega(t) \to 0$ as $t \to \infty$, and $\dot{\omega}(t) \to 0$, as $t \to \infty$. Considering these with the definitions of $\delta_3(t)$, and $\delta_4(t)$ from (53) and (54) respectively, leads to the conclusion that both $\delta_3(t)$, and $\delta_4(t)$ tend to zero as $t \to \infty$. Further the term $\left(\frac{\hat{K}_t(t)i_a(t)}{\hat{J}(t)}\right) = \left(\frac{i_a(t)}{\hat{J}(t)/\hat{K}_t(t)}\right)$. Now, from Lemma 4.1 it is known that $\left(\hat{J}(t)/\hat{K}_t(t)\right) > 0$, and also by assumptions, $i_a(t) \to 0$ as $t \to \infty$. So this implies that $\left(\frac{\hat{K}_t(t)i_a(t)}{\hat{J}(t)}\right) \to 0$ as $t \to \infty$. Therefore, it is possible to say that the terms $\int_{t_0}^{t}\delta_3^2(\tau)d\tau$, $\int_{t_0}^{t}\delta_4^2(\tau)d\tau$, and $\int_{t_0}^{t}\left(\frac{\hat{K}_t(\tau)i_a(\tau)}{\hat{J}(\tau)}\right)^2 d\tau$ in (63) and (71) are bounded. Further suppose that at some time $t^* > t_0$, $e_2(t)$ is either positive or negative. Now suppose $k_2(t) \to \infty$ as $t \to \infty$, then according to (4), the Nussbaum function can take values at $+\infty$, and this will violate positiveness of the L.H.S in both (63) and (71). Thus, by contradiction, $k_2(t)$ is bounded. Also, from (13), $k_2(t)$ is an increasing function. Thus, the above facts imply that $k_2(t) \to k_{2\infty}$ as $t \to \infty$, which indicates that as $t \to \infty$, $\dot{k}_2(t) \to 0$ i.e. $e_2^2(t) \to 0$ or $e_2(t) \to 0$. Thus, from (12), this results in $\hat{\omega}(t) \to \omega(t)$, i.e. $\dot{\hat{\omega}}(t) \to \dot{\omega}(t)$ as $t \to \infty$. So, from (2) and (7),

$$\frac{\hat{K}_t(t)i_a(t)}{\hat{J}(t)} - \frac{\hat{b}(t)\hat{\omega}(t)}{\hat{J}(t)} + u_2(t) = \frac{K_t i_a(t)}{J} - \frac{b\omega(t)}{J} \tag{72}$$

Because $e_2(t) \to 0$, and from Gorenflo and Mainardi (1996) and Li and Chen (2009) it is known that $N(k_2(t))$ approaches some constant value as $k_2(t) \to k_{2\infty}$, so $u_2(t) = N(k_2(t))e_2(t) \to 0$, and $\hat{\omega}(t) \to \omega(t)$ as $t \to \infty$. Eq. (72) can be written as

$$\begin{bmatrix}\left(\frac{K_t}{J} - \frac{\hat{K}_t(t)}{\hat{J}(t)}\right) & \left(\frac{\hat{b}(t)}{\hat{J}(t)} - \frac{b}{J}\right)\end{bmatrix}\begin{bmatrix}i_a(t)\\ \omega(t)\end{bmatrix} = 0 \tag{73}$$

Now by assumption $i_a(t) \ne 0$ and $\omega(t) \ne 0$. Therefore, it can be inferred from (73) that as $t \to \infty$

$$\frac{\hat{K}_t(t)}{\hat{J}(t)} = \frac{K_t}{J} \tag{74}$$

$$\frac{\hat{b}(t)}{\hat{J}(t)} = \frac{b}{J} \tag{75}$$

Thus proving the required results. □

Having proven the main results required, the assumptions made in the above theorems, robustness to effects of noise, requirement/non-requirement of the well known persistence of excitation (PE) condition, are discussed first. Following this, another result is provided, which shows that the parameters estimated by the proposed adaptive motor parameters estimation strategy actually converge.

Remark 2. The assumptions made about the motor input voltage $E(t)$, motor current $i_a(t)$, and the motor speed $\omega(t)$, in Theorems 4.2 and 4.3 are not hard to meet. All that is needed, is to have a gradually (and smoothly) declining motor input terminal voltage. This is easily achieved by charging an appropriate capacitor bank and, then letting the capacitor bank discharge through the motor. As the capacitor bank discharges, the terminal voltage declines smoothly, and this also leads the motor current and the speed to decline smoothly and gradually. To meet the assumption that $i_a(t), \omega(t), E(t)$ all tend to zero but are not equal to zero, it is possible to just use parts of the motor current, motor speed, and input voltage vs. time curves where these quantities are very small but are not zero. Also, conducting such a test does not need a large amount of time, so whenever motor parameters need to be updated, a test as mentioned above using capacitor banks, can be easily performed to quickly update motor parameters. Also, it is not critically necessary to have a motor on no-load as explained at the end of Section 5.3.

In Mukhopadhyay et al. (2008), a series of rigorous experiments are performed on a DC motor using UAS for robust and real-time control applications. Also in Ali et al. (2017), a UAS based adaptive observer is used to estimate Li-ion battery parameters, and results are verified across charging and discharging tests for 16 different batteries. And in Al Khatib et al. (2015), a UAS based strategy is used for robot motion control, and is tested by injecting noise, Al Khatib et al. (2015) also provides some strategies to combat these effects. These results show that the proposed UAS based adaptation strategy ensures convergence and, thus, guarantees accurate parameters estimation in the presence of sensor noise or external disturbances. Further, gain-management techniques known from literature on classical adaptive control can be used, like in Al Khatib et al. (2015) to combat such effects. While a fully detailed analysis of the effects of noise is out of the scope of the current work, the authors have performed some preliminary analysis and provide a sketch of a proof as follows. If the current, speed measurements in this paper are considered to have an additive bounded offset (i.e. noise or disturbance), then following the steps in the results in this paper which include disturbance terms like $\delta_1, \delta_2, \delta_3, \delta_4$, it is possible to lump the effects of noise or other external disturbances within $\delta_1, \delta_2, \delta_3, \delta_4$. Then it is possible to arrive at a conclusion that as long as such noise/disturbance terms, and their derivatives are bounded (which is the case for any physical disturbance or noise), then all further steps as in Theorems 4.2, 4.3 still hold, providing the required results. Another approach to deal with noise and disturbance may be as follows. This technique needs $E(t) \to 0$, i.e. this corresponds to the situation when a motor is being temporarily shut-off for maintenance and the motor has not stopped but is about to stop. This leads to decaying curves for motor voltage, current, and speed, with characteristic time constants. In this situation, eliminating noise, or disturbances is very simply possible by adding a low-pass filter, or a moving average mechanism before proceeding with adaptive parameter estimation.

The previous work in Ali et al. (2017) and Usman et al. (2018), and this work, use UAS based techniques for parameters estimation. As observed from the results, reasonably accurate parameter estimates are obtained without any explicit imposition of the PE condition. A small discussion of this is available in the penultimate paragraph in Section 1, to which readers are directed.

Lemma 4.4. *Suppose $\lambda_{xn}, \lambda_{yn}, z_{nu}$ and z_{nl} are positive real numbers, where $n \in \{1, \dots, 6\}$. If all conditions required for Theorems 4.2 and 4.3 to hold are satisfied, then for all $n \in \{1, 2, \dots, 6\}$, $\hat{z}_n(t)$ converges to some constant $z_{n\infty}$, as $t \to \infty$.*

Proof. The solution of (16) with $e^2(t) + \lambda_{xn} z_{nu} + \lambda_{yn} z_{nl}$ as an input is as follows

$$\hat{z}_n(t) = \hat{z}_n(t_0) e^{-(\lambda_{xn}+\lambda_{yn})t} + \int_{t_0}^{t} e^2(t-\tau) e^{-(\lambda_{xn}+\lambda_{yn})\tau} d\tau + (\lambda_{xn} z_{nu} + \lambda_{yn} z_{nl}) \int_{t_0}^{t} e^{-(\lambda_{xn}+\lambda_{yn})\tau} d\tau. \tag{76}$$

It is known from (17), and (18) that, $e(t) = e_1(t)$ for $n \in \{1, 2, 3\}$ and $e(t) = e_2(t)$ for $n \in \{4, 5, 6\}$. Because $e^{-(\lambda_{xn}+\lambda_{yn})t} \to 0$ as $t \to \infty$, and also from Theorems 4.2 and 4.3, $e_1(t) \to 0$, and $e_2(t) \to 0$ as $t \to \infty$. Thus, on the R.H.S of (76), the first term goes to zero, and second and third terms are bounded and approach some constant value as $t \to \infty$. Hence, $\hat{z}_n(t)$ converges to some constant $\hat{z}_{n\infty}$, as $t \to \infty$ for all $n \in \{1, \dots, 6\}$. □

Thus all the above results show that the proposed parameters estimation strategy converges. The accuracy of the estimates obtained is discussed next.

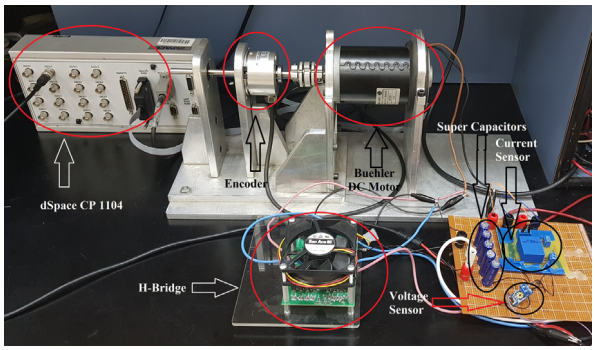

Fig. 4. Experimental setup for PMDC motor.

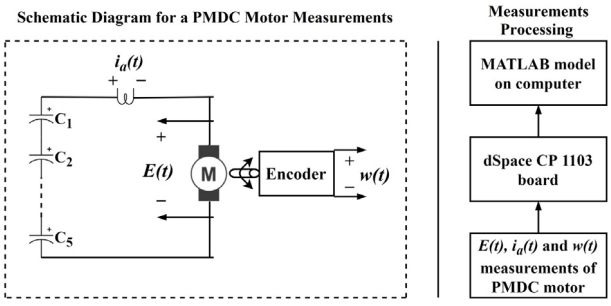

Fig. 5. Schematic diagram, and PMDC motor measurements process flow.

4.1. Expected accuracy of estimated motor parameters

Though inappropriate selection of the values for the bounds z_{nu} and z_{nl}, and noise in the data collected during experimentation may cause errors in the estimated PMDC motor parameter values, the following considerations can help gauge the amount of inaccuracy possible, or the ease with which the above mentioned problems can be avoided. First, to get appropriate values of bounds z_{nu} and z_{nl}, a motor's datasheet may be used, with bound values z_{nu}, z_{nl} picked to be around $\pm 10\%$ respectively of the corresponding parameter value in the datasheet. Second, noisy inputs/data can be easily pre-filtered before being fed to the proposed adaptive parameter estimator. And third, consider the following simple analysis of errors in parameters estimation. Suppose $\hat{K}_t(t) = K_t(t) + \Delta_1$, where Δ_1 is some small error term due to the above mentioned reasons. Substituting the value of $\hat{K}_t(t)$ in (74) gives $\hat{J}(t) = J(t)\left(1 + \frac{\Delta_1}{K_t(t)}\right)$ or $\hat{J}(t) = J(t) + \Delta_2$. If the upper and lower bounds on $\hat{K}_t$ are known somewhat accurately, then it is possible to have Δ_1 several orders of magnitude smaller than the order of magnitude of K_t. Getting reasonably accurate upper and lower bounds for K_t are not hard because one simply needs the no-load torque per ampere, which can be easily measured, or is readily available in a datasheet. Please notice that $\Delta_2 < \Delta_1$ as $\Delta_2 = \frac{J(t)}{K_t(t)}\Delta_1$ and generally the value of $\frac{J(t)}{K_t(t)} < 1$ with the motor having no load. Similarly using $\hat{J}(t) = J(t) + \Delta_2$ in (75) gives $\hat{b}(t) = b(t)\left(1 + \frac{\Delta_2}{J(t)}\right)$ or $\hat{b}(t) = b(t) + \Delta_3$. Also, notice that $\Delta_3 < \Delta_2$, as $\Delta_3 = \frac{b(t)}{J(t)}\Delta_2$ and the value of $\frac{b(t)}{J(t)} < 1$ with order of magnitude mostly in the range of 10^{-3}. Therefore, $\Delta_3 < \Delta_2 < \Delta_1$, i.e. the parameters estimation error in $\hat{J}(t)$ and $\hat{b}(t)$ is less than the parameter estimation error in $\hat{K}_t(t)$. And as shown in Theorem 4.2 the estimates $\hat{L}_a, \hat{R}_a, \hat{K}_b$ converge to the actual values, which confirms that the proposed strategy estimates the PMDC motor parameters with reasonable accuracy.

5. Experimental verification of the proposed parameters estimation methodology

In this section, the proposed parameters estimation algorithm is validated, on a 24 V, 3200 RPM (335.1 rad/s) PMDC motor. Section 5.1

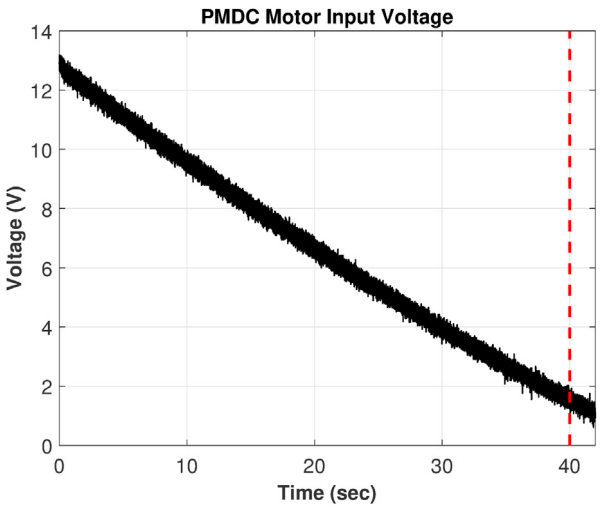

Fig. 6. PMDC motor input voltage during adaptive estimation process.

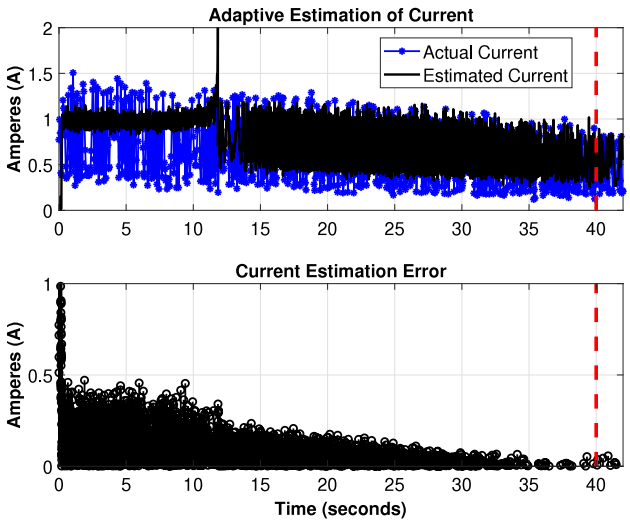

Fig. 7. Comparison of estimated and actual current of PMDC motor during adaptive estimation process.

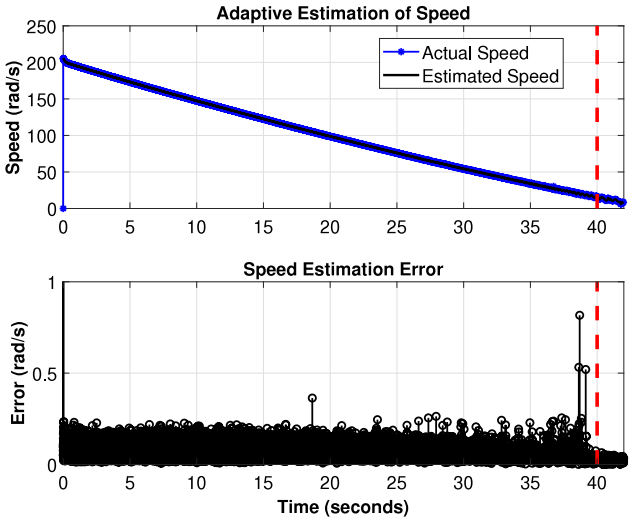

Fig. 8. Comparison of estimated and actual speed of PMDC motor during adaptive estimation process.

describes the hardware setup used for PMDC motor parameters estimation and experimentation. In Section 5.2, the parameters of the PMDC motor are estimated using the proposed UAS based adaptive parameters estimation method. The estimated parameters $\hat{z}_1, \ldots, \hat{z}_6$ are recorded when the estimated speed and current errors of the PMDC motor approach a small value. Lastly in Section 5.3, the estimated parameters are then used to further estimate the speed of the 24 V, 3200 RPM PMDC motor. The accuracy of estimated parameters is quantified by comparing the estimated speed with the actual speed of the PMDC motor.

5.1. PMDC hardware setup

The experiments are performed on a "Buehler brushed PMDC motor, model no. 1.13.075.214" (Bühler Motor, 2010). As discussed in Section 4 the motor current $i_a(t) \to 0$ and motor speed $\omega(t) \to 0$ as $t \to \infty$, are required by the UAS based adaptive parameters estimation process to ensure accurate parameters estimation. The conditions $i_a(t) \to 0$ and $\omega(t) \to 0$ as $t \to \infty$, are satisfied by supplying a decaying input voltage to the PMDC motor. For this purpose, five super capacitors rated at 2.5 V, 10 F are used in series to produce an overall capacitor bank rated at 12.5 V, and 2 F. The voltage profile of these five series connected super capacitors, connected with the PMDC motor is shown in Fig. 6. The capacitor bank is fully charged at the beginning of each test. Note that, the PMDC motor is operated without any load for the experiments.

Voltage sensors, current sensors, and an encoder along with a dSPACE CP 1104 DAQ board are used for data acquisition as shown in Figs. 4 and 5. The schematic diagram and PMDC motor measurements process flow is shown in Fig. 5. The voltage, current, and speed of the PMDC motor are recorded, and these measurements are then utilized for current and speed estimation of the PMDC motor.

5.2. UAS based PMDC motor adaptive parameters estimation

Equation (16) is used to estimate the PMDC motor parameters $\hat{z}_1, \ldots, \hat{z}_6$. The adaptive equation (16) requires an initial value, upper and lower bounds and their respective confidence levels for each parameter. The initial values, upper and lower bounds and their respective confidence levels based on the manufacturer provided datasheet, are given in Table 2. Note that the selection of initial values, upper and lower bounds and their respective confidence levels for parameters $\hat{L}_a$, $\hat{R}_a$, $\hat{b}$, and $\hat{J}$ should be in accordance with the conditions described in Lemma 4.1.

The parameters $\hat{R}_a, \hat{K}_b$, and $\hat{L}_a$, estimated by (16), along with the actual PMDC motor voltage and speed are used in (6) to estimate the motor current. The parameters $\hat{J}, \hat{K}_t$, and $\hat{b}$, estimated by (16), along with the actual PMDC motor current is used in (7) to estimate the motor speed. The error in the estimated current is fed back into (16) and (6). While the error in the estimated speed is fed back into (16) and (7). Eqs. (6) and (7) describe the high gain adaptive parameters estimator used for PMDC motor parameters estimation. Equation (16) tunes all the six parameters $\hat{z}_1, \ldots, \hat{z}_6$ to bring the current and speed estimation error to zero. When the current and speed estimation errors go to zero, i.e. $e_1(t) \to 0$ and $e_2(t) \to 0$ as $t \to \infty$, the estimated motor parameters values converge to the actual motor parameters values.

The comparison of estimated and actual PMDC motor current, and current estimation error, is shown in Fig. 7. Note that $e_1(t)$ is the current estimation error. Because the PMDC motor is operated at no-load condition, the motor draws a small current. The decaying current profile of the PMDC motor is seen in the upper half of Fig. 7. After 40 s, it is observed that $e_1(t) \to 0$ as $t \to \infty$, as in the lower half of Fig. 7. As per algorithm 1, it is after this time instant that some of the motor parameters i.e. $\hat{L}_a$, $\hat{R}_a$, $\hat{K}_b$ are estimated. Similarly, the comparison of

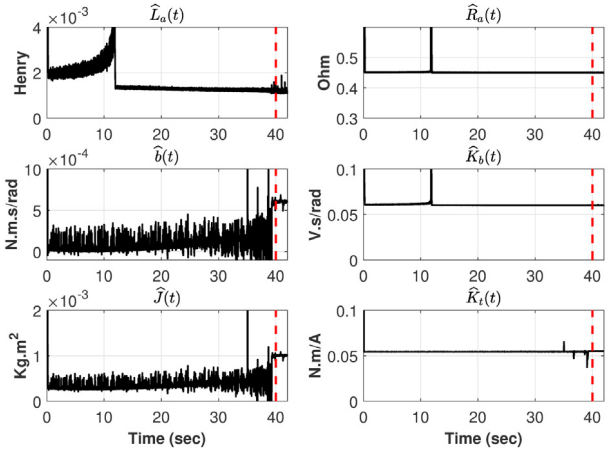

Fig. 9. Variation of PMDC motor parameters during adaptive estimation process.

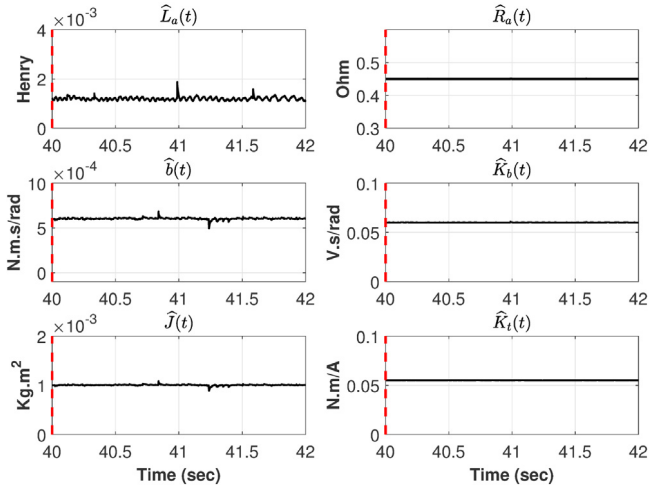

Fig. 10. Zoomed version of variation of PMDC motor parameters during adaptive estimation process after 40 seconds.

estimated and actual PMDC motor speed, and speed estimation error are given in Fig. 8. Also $e_2(t)$ represents the speed estimation error. The decaying speed profile of the PMDC motor is seen in the upper half of Fig. 8. Just as in the case of current estimation, similarly at a time instant after 40 s the speed estimation error, i.e. $e_2(t) \to 0$ as $t \to \infty$, which can be observed in the lower half of Fig. 8. And, as per algorithm 1, it is after this time instant that the remaining motor parameters i.e. $\widehat{J}$, $\widehat{b}$, $\widehat{K}_t$ are estimated. The effectiveness of Mittag-Leffler (ML) function as a Nussbaum function for parameter estimation purposes is quantified by showing the current and speed estimation error comparison between UAS based motor parameters estimation with the ML function as Nussbaum function, and UAS based motor parameters estimation with other Nussbaum functions. The details are in Table 1. Here $N_1(k)$ denotes a Mittag-Leffler function as a Nussbaum function, whereas $N_2(k)$ and $N_3(k)$ are derived from Ilchmann (1993). The results in Table 1 suggest that using a ML function as a Nussbaum function ensures fast and accurate convergence of current and speed estimates compared to other types of Nussbaum functions, when used with the UAS based parameters estimation strategy proposed in this paper. The variations of PMDC motor parameters during the adaptive estimation process are recorded and shown in Fig. 9. The convergence of PMDC motor parameters can be seen in Fig. 9 after 40 s when $e_1(t) \to 0$ in Fig. 7, and $e_2(t) \to 0$ in Fig. 8. The zoomed version of PMDC motor parameters after 40 s are also shown in Fig. 10. During this period, i.e. after 40 s when $e_1(t) \to 0$, and $e_2(t) \to 0$, the mean value of each individual estimated parameter gives the estimated PMDC motor parameter value, as per the Algorithm 1. Furthermore, three different sets of parameters are formed, which are defined as follows.

- Set 1 (S1): This set includes the PMDC motor parameters estimated by using the proposed UAS based adaptive parameters estimation method.
- Set 2 (S2): The PMDC motor parameters obtained through direct experimentation (not using the proposed adaptive parameters estimation method), are kept in this set.
- Set 3 (S3): This set contains the data sheet parameters of the PMDC motor.

The estimated parameters (S1) and the parameters given in the data sheet (S3) of the PMDC motor are given in Table 2. The PMDC motor parameters obtained through direct experimentation (S2) are also provided in Table 2. It is worth mentioning that there are standard procedures, and practices available in the literature for direct experimentation based motor parameters estimation. Next, steps quantify the accuracy of adaptively estimated parameters (S1), experimentally obtained parameters (S2) and the parameters given in data sheet (S3) by comparing DC motor speed estimated using the parameters in sets S1, S2, S3 mentioned above, with the actual speed of the PMDC motor.

5.3. Accuracy assessment of PMDC motor parameters via speed response comparison

The Set 1 (S1), Set 2 (S2) and Set 3 (S3) parameters are used in PMDC motor equations (1)–(2) to get speed estimates corresponding to parameters from each set. First, the speed response when the PMDC motor is excited with the rated 24 V step input voltage is analyzed. The step input voltage is applied to the PMDC motor after 3 s and the speed responses using S1, S2, and S3 parameters are compared in Fig. 11. The steady state speed estimation error using the S1, and S2 parameters is less than 1%, and it is 9% when using S3 parameters.

The speed responses using S1, S2 and S3 parameters are analyzed with respect to their speed estimation error while applying the rated ± 24 V as shown in Fig. 12. The polarity of the rated 24 V supply is reversed in a periodic manner, i.e the rated voltage is applied at both polarities with a time period of 5 s. The steady state error analysis in this case, is similar to that of Fig. 11.

Further the estimated speed and speed estimation error using S1, S2 and S3 parameters, are compared for randomly varying input voltage. This randomly varying input voltage is the combination of step and ramp voltages and is shown in Fig. 13. The speed response using set S1, S2 and S3 parameters with their speed estimation errors are also shown in Fig. 13. The maximum and average of absolute percentage

Table 1
Comparison of average absolute current and speed estimation errors during adaptive parameters estimation using different Nussbaum functions.

Estimation error after 40 s	$N_1(k(t)) = E_a(-k(t)^\alpha)$	$N_2(k(t)) = k(t)^2 cos(k(t))$	$N_3(k(t)) = k(t) cos(\sqrt{\lvert k(t)\rvert})$
Average absolute current estimation error (A)	0.1052	0.19	0.7407
Average absolute speed estimation error (rad/s)	0.0078	0.0686	0.1175

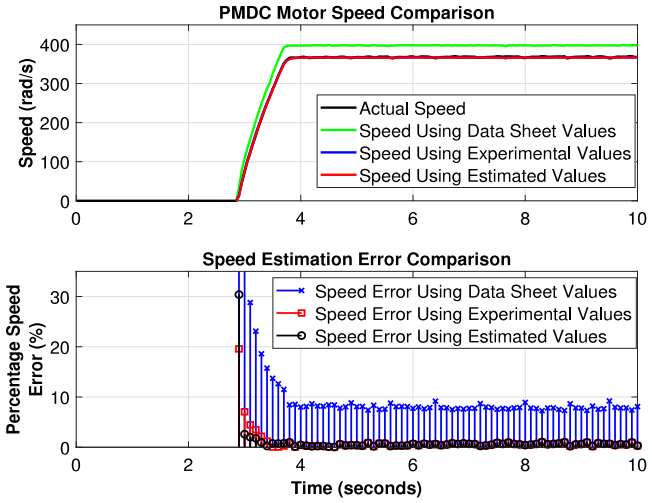

Fig. 11. Step response of speed, and absolute percentage speed error comparison of PMDC motor.

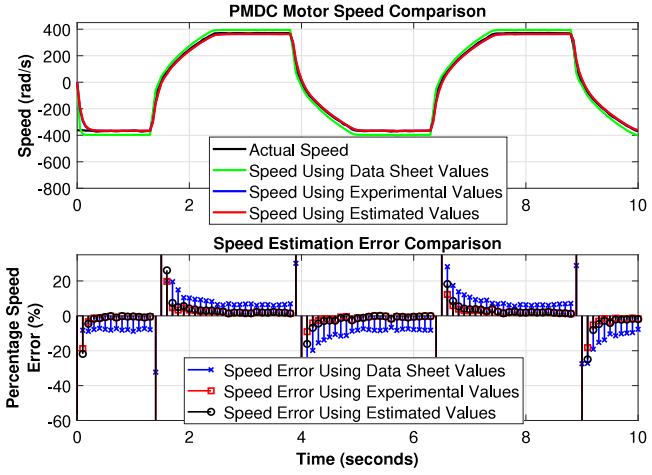

Fig. 12. Step response of speed and percentage speed error comparison of PMDC motor with periodic input voltage sign reversal.

speed error during random input excitation of PMDC motor in Fig. 13, are given in Table 3.

The wear and tear of a PMDC motor causes higher speed estimation error when data sheet parameter values are used. Therefore, the proposed UAS based adaptive estimation strategy is robust to the parameters variation due to motor aging, and it can be used to update PMDC motor parameters with high accuracy, and by collecting data for only a single experimental run.

The conditions imposed by Theorems 4.2 and 4.3 for parameters estimation, i.e. $E(t) \to 0$, $i(t) \to 0$, and $\omega(t) \to 0$ are not hard to meet and can be satisfied even for loaded PMDC motor operation. The proposed method is feasible for real-time parameters estimation of a

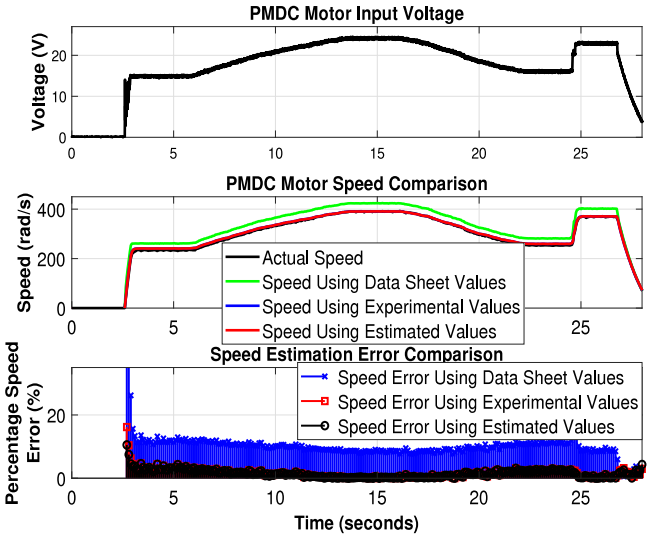

Fig. 13. Speed response and absolute percentage speed error comparison of PMDC motor with random input excitation.

PMDC motor regardless of any loading condition. Because PMDC motor parameters are load invariant, as presented by results in Sankardoss and Geethanjali (2017), the parameters estimated at no-load or at any load are similar. Further, as described in the introduction, a motivation of this work is a strategy which allows quick re-estimation of parameters as needed during a motor's operational life. It is completely feasible to assume that any motor in any application does not run continuously forever. There have to be some instances over the life of a motor, where there are some breaks in operation, i.e. a motor is shut-off for routine maintenance. All that is needed then, is embedding an adaptive algorithm, as the one proposed in this work, to operate during such above instances of breaks in operation, where the required conditions are satisfied. Further, for a PMDC motor operating at any loading condition, turning off the supply voltage to stop the motor operation causes the PMDC motor rotor current and speed to decay to zero. The current and speed decay time depends on electrical and mechanical time constants, respectively, which are mostly in the range of few milliseconds. In this duration, when the supply voltage of a PMDC motor is reducing to zero, the voltage, current and speed data can be recorded using sensors at a high sampling rate. Collecting the data at a high sampling rate provides sufficient data points to execute the proposed UAS based adaptation strategy for parameters estimation. Thus, reducing the supply voltage $E(t)$ to zero, for any loaded/unloaded PMDC motor, will eventually reduce the motor speed $\omega(t)$ and current $i(t)$ to zero before dying out. And this data recorded in the duration (before motor speed $\omega(t)$ and current $i(t)$ die out) satisfy all the conditions described in Theorems 4.2 and 4.3, i.e. $E(t) \to 0$, $i(t) \to 0$, and $\omega(t) \to 0$ as $t \to \infty$.

Table 2
Experimental and adaptively estimated results of PMDC motor parameters.

Parameter	Unit	Initial value	Upper bound (z_{nu})	Lower bound (z_{nl})	Upper bound confidence λ_{xn}	Lower bound confidence λ_{yn}	Set 1 (S1) estimated value	Set 2 (S2) experimental values	Set 3 (S3) data sheet values
L_a	mH	1	2	0.2	55	55	1.2	1	0.9
R_a	Ω	10	0.8	0.1	45	45	0.4501	0.5882	0.45
J	kg m^2	1	20e−4	1e−6	40	40	5.13e−4	2.52e−4	1.8e−4
b	N m s/rad	0.5	12e−4	1e−6	50	50	2.11e−4	1.73e−4	5.22e−6
K_t	N m/A	1	0.1	0.01	50	50	0.0546	0.0385	0.057
K_b	V s/rad	1	0.11	0.01	50	50	0.0601	0.0592	0.057

Table 3
Speed estimation error analysis, with random input excitation as shown in Fig. 13.

Set of parameters used	Maximum absolute error (%)	Average absolute error (%)
Estimated values (S1)	9.6219	1.3098
Experimental values (S2)	8.1358	1.3466
Data sheet values (S3)	19.9215	8.4235

6. Conclusion

An adaptive and experimentally less demanding Permanent Magnet DC (PMDC) motor parameters estimation strategy has been developed and validated in this work. The proposed strategy uses a high gain adaptive estimator. The motor current and speed estimation errors are used in the adaptive estimation process to accurately estimate PMDC motor parameters in a single experimental run. The results show the effectiveness of the proposed method, and thus show that this method can help to quickly achieve an accurate set of motor parameter values regardless of wear and tear of a PMDC motor. The proposed UAS based parameters adaptation technique can be very helpful for the accurate monitoring and control of a PMDC motor. The proposed algorithm is verified experimentally in the presence of sensor noise, and the strategy provides accurate estimation of PMDC motor parameters even without imposing the persistence of excitation (PE) condition. The results achieved are for motor operation on no-load, and investigation of the effects of load on the technique developed, are left for future work. Future extensions of this work may also include techniques to select the upper, lower bounds, initial values, and confidence values required for the algorithm. Investigation into the requirement/non-requirement of the PE criteria with an algorithm of the type proposed in this paper, is also left for future efforts.

Acknowledgments

Parts of this work were funded via grant number FRG17-R-34 received from the Office of Research and Graduate studies at the American University of Sharjah, UAE.

Declaration of competing interest

None declared.

References

Al Khatib, E. I., Al-Masri, W. M., Mukhopadhyay, S., Jaradat, M. A., & Abdel-Hafez, M. (2015). A comparison of adaptive trajectory tracking controllers for wheeled mobile robots. In *2015 10th International Symposium on Mechatronics and its Applications (ISMA)* (pp. 1–6). IEEE.

Ali, D., Mukhopadhyay, S., Rehman, H., & Khurram, A. (2017). UAS based Li-ion battery model parameters estimation. *Control Engineering Practice*, *66*, 126–145. http://dx.doi.org/10.1016/j.conengprac.2017.06.012.

Alkhawaja, F., Koirala, K., Daffalla, M., Kassem, M., Tily, M. A., Al-Rousan, G., et al. (2018). Experimental verification of UAS based battery terminal voltage collapse detection on a simple embedded platform. In *2018 11th International Symposium on Mechatronics and its Applications (ISMA)* (pp. 1–6).

Aranovskiy, S., Bobtsov, A., Ortega, R., & Pyrkin, A. (2017). Performance enhancement of parameter estimators via dynamic regressor extension and mixing. *IEEE Transactions on Automatic Control*, *62*(7), 3546–3550.

Belov, A., Aranovskiy, S., Ortega, R., Barabanov, N., & Bobtsov, A. (2018). Enhanced parameter convergence for linear systems identification: the DREM approach. In *2018 European Control Conference (ECC)* (pp. 2794–2799). IEEE.

Bühler Motor (2010). Büehler motor product range 2010. [Online] Available: http://www.oem.co.uk/products/Motors.

Da Silva, M. F., Bastos, F. F., Da Silva Casillo, D. S., & Casillo, L. A. (2016). Parameters identification and analysis of brushless direct current motors. *IEEE Latin America Transactions*, *14*(7), 3138–3143.

Galijašević, S., Mašić, Š., Smaka, S., Akšamović, A., & Balić, D. (2011). Parameter identification and digital control of speed of a permanent magnet DC motors. In *23rd IEEE International Symposium on Information, Communication and Automation Technologies (ICAT)*.

Gorenflo, R., & Mainardi, F. (1996). Fractional Oscillations and Mittag-Leffler Functions. [Online] Available: ftp://ftp.math.fu-berlin.de/pub/math/publ/pre/1996/pr-a-96-14.ps.

Hadef, M., Bourouina, A., & Mekideche, M. (2008). Parameter identification of a DC motor via moments method. *Iranian Journal of Electrical and Computer Engineering*, *7*(2), 159–163.

Hernández-Márquez, E., Silva-Ortigoza, R., García-Sánchez, J. R., Marcelino-Aranda, M., & Saldaña-González, G. (2018). A DC/DC buck-boost converter–inverter–DC motor system: Sensorless passivity-based control. *IEEE Access*, *6*, 31486–31492.

Ilchmann, A. (1993). *Lecture notes in control and information sciences: vol. 189, Non-identifier-based high-gain adaptive control*. Springer-Verlag.

Li, Y., & Chen, Y. (2009). When is a Mittag–Leffler function a Nussbaum function? *Automatica*, *45*(8), 1957–1959.

Mamani, G., Becedas, J., Feliu-Batlle, V., & Sira-Ramirez, H. (2007). Open-loop algebraic identification method for a DC motor. In *IEEE European Control Conference (ECC)* (pp. 3430–3436).

Mathai, A. M., & Haubold, H. J. (2008). *Special functions for applied scientists, Vol. 4*. Springer.

Mukhopadhyay, S. (2008). Mittag-Leffler function, M-file, cmex DLL, and S-function - File Exchange - MATLAB Central. [Online] Available: https://www.mathworks.com/matlabcentral/fileexchange/20731-mittag-leffler-function--m-file--cmex-dll--and-s-function?requestedDomain=true.

Mukhopadhyay, S., Li, Y., & Chen, Y. (2008). Experimental studies of a fractional order universal adaptive stabilizer. In *2008 IEEE/ASME International Conference on Mechtronic and Embedded Systems and Applications* (pp. 591–596). IEEE.

Mukhopadhyay, S., & Zhang, F. (2014). A high-gain adaptive observer for detecting Li-ion battery terminal voltage collapse. *Automatica*, *50*(3), 896–902. http://dx.doi.org/10.1016/j.automatica.2013.12.011.

Na, J., Xing, Y., & Costa-Castelló, R. (2018). Adaptive estimation of time-varying parameters with application to roto-magnet plant. *IEEE Transactions on Systems, Man, and Cybernetics: Systems*, 1–11. http://dx.doi.org/10.1109/TSMC.2018.2882844.

Ortega, R., Bobtsov, A., Pyrkin, A., & Aranovskiy, S. (2015). A parameter estimation approach to state observation of nonlinear systems. *Systems & Control Letters*, *85*, 84–94.

Ortega, R., Praly, L., Aranovskiy, S., Yi, B., & Zhang, W. (2018). On dynamic regressor extension and mixing parameter estimators: Two Luenberger observers interpretations. *Automatica*, *95*, 548–551.

Puangdownreong, D., Hlungnamtip, S., Thammarat, C., & Nawikavatan, A. (2017). Application of flower pollination algorithm to parameter identification of DC motor model. In *IEEE International Electrical Engineering Congress (IEECON)* (pp. 1–4).

Rodríguez-Molina, A., Villarreal-Cervantes, M. G., Álvarez-Gallegos, J., & Aldape-Pérez, M. (2019). Bio-inspired adaptive control strategy for the highly efficient speed regulation of the dc motor under parametric uncertainty. *Applied Soft Computing*, *75*, 29–45.

Rubaai, A., & Kotaru, R. (2000). Online identification and control of a DC motor using learning adaptation of neural networks. *IEEE Transactions on Industry Applications*, *36*(3), 935–942.

Sankardoss, V., & Geethanjali, P. (2017). PMDC motor parameter estimation using bio-inspired optimization algorithms. *IEEE Access*, *5*, 11244–11254.

Sastry, S. (1999). *Nonlinear systems, analysis, stability, and control*. Springer.

Sendrescu, D. (2012). Parameter identification of a DC motor via distribution based approach. In *17th IEEE International Conference on Methods and Models in Automation and Robotics (MMAR)* (pp. 17–22).

Silva-Ortigoza, R., Hernández-Guzmán, V. M., Antonio-Cruz, M., & Munoz-Carrillo, D. (2015). DC/DC buck power converter as a smooth starter for a dc motor based on a hierarchical control. *IEEE Transactions on Power Electronics*, *30*(2), 1076–1084.

Sun, X., Li, S., Li, P., Shi, X., & Hu, S. (2015). Research on adaptive identification methods for time-variant parameters of rare earth brushless DC motors. In *27th IEEE Chinese Control and Decision Conference (CCDC)* (pp. 6472–6475).

Usman, H. M., Mukhopadhyay, S., & Rehman, H. (2018). Universal adaptive stabilizer based optimization for Li-ion battery model parameters estimation: An experimental study. *IEEE Access*, *6*, 49546–49562.

Wu, W. (2010). DC motor identification using speed step responses. In *IEEE American Control Conference (ACC)* (pp. 1937–1941).

Yi, B., Ortega, R., & Zhang, W. (2018). Relaxing the conditions for parameter estimation-based observers of nonlinear systems via signal injection. *Systems & Control Letters*, *111*, 18–26.